BANK OF GREECE
EUROSYSTEM

Working Paper

Trend inflation and inflation expectations in high dimensional vector autoregressions

Dimitrios P. Louzis

360

MARCH 2026

BANK OF GREECE
Economic Analysis and Research Department – Special Studies Division
21, E. Venizelos Avenue
GR-102 50 Athens
Tel: +30210-320 3610
Fax: +30210-320 2432

www.bankofgreece.gr

Published by the Bank of Greece, Athens, Greece

ISSN: 2654-1912 (online)
DOI: https://doi.org/10.52903/wp2026360

TREND INFLATION AND INFLATION EXPECTATIONS IN HIGH DIMENSIONAL VECTOR AUTOREGRESSIONS

Dimitrios P. Louzis

Bank of Greece

ABSTRACT

This paper introduces a new class of large vector autoregression (VAR) models with a hybrid trend structure that explicitly incorporates both trend inflation and inflation expectations, proxied by long-term survey forecasts and statistical filters. We develop efficient Bayesian estimation methods leveraging recent advances in matrix precision algorithms, substantially reducing computational costs and enabling large-scale forecasting exercises. Using a dataset of 20 U.S. macroeconomic variables, we show that incorporating trend inflation and survey-based expectations within a high-dimensional VAR framework markedly improves inflation forecast accuracy relative to widely used large-VAR benchmarks.

Keywords: Inflation Forecasting; Survey-Based Inflation Expectations; Large-Cross Section; Efficient MCMC algorithms

JEL classification: E31; E37; C51; C53; C55

Disclaimer: The author would like to thank Michele Modugno, Marta Bańbura, and participants at the CRETE 2023 Conference and the WGF 2024 Workshop (Athens) for helpful comments and suggestions. The views expressed in this paper are those of the author and do not necessarily reflect the views of the Bank of Greece. Any remaining errors or omissions are the sole responsibility of the author.

Correspondence:
Dimitrios Louzis
Economic Analysis and Research Department
Bank of Greece
El.Venizelos 21, 10250 Athens, Greece
Tel.: +30-2103202648
email: dlouzis@bankofgreece.gr

1 Introduction

Measuring and forecasting inflation accurately is central to the conduct of credible monetary policy. Central banks routinely produce macroeconomic and inflation forecasts that play a decisive role in determining their policy stance. Consequently, the importance of inflation forecasting has long motivated both academic research and policy institutions to develop econometric models capable of producing reliable inflation forecasts (see e.g. Faust & Wright, 2013, and references therein). More recently, the worldwide inflationary pressures observed in the aftermath of the COVID-19 pandemic have renewed interest in this area. Researchers have revisited the ability of well-established models to forecast inflation, such as the Phillips curve framework (see e.g. Bańbura & Bobeica, 2022, and references therein), while also proposing modern computationally intensive approaches that exploit the informational content of large datasets (see e.g. Hauzenberger, Huber, & Klieber, 2023, and references therein).

Following the seminal contribution of Bańbura, Giannone, and Reichlin (2010), large vector autoregression (VAR) models have become a standard tool in macroeconomic forecasting. The macroeconometric literature has largely concluded that exploiting the informational content of large datasets of macroeconomic and financial variables, combined with an appropriate degree of Bayesian shrinkage, improves macroeconomic—and particularly inflation—forecasting performance (see e.g. Bańbura et al., 2010; Carriero, Clark, & Marcellino, 2015, 2016a, 2019; Koop & Korobilis, 2013; Giannone, Lenza, & Primiceri, 2015; Chan, 2020a, 2020b, 2022, among others). Another strand of the VAR literature emphasizes the importance of modeling the unconditional mean of the data-generating process in order to enhance forecasting performance. Existing empirical evidence suggests that both informative steady-state priors and specifications that allow for time-varying unconditional means or trends can substantially improve the forecasting performance of VAR models (see e.g. Villani, 2009; D. Louzis, 2016b; D. P. Louzis, 2019; Banbura & van Vlodrop, 2018; Banbura, Brenna, Paredes, & Ravazzolo, 2021; Banbura, Leiva-Leon, & Menz, 2021).

Focusing more specifically on inflation modeling and forecasting, several studies highlight the importance of trend inflation within unobserved component (UC) frameworks. In particular, Stock and Watson (2007), Chan, Koop, and Potter (2013), Chan, Koop, and Potter (2016), and Chan, Clark, and Koop (2018) emphasize the role of trend inflation in improving inflation forecasts using univariate and bivariate UC models. Notably, Chan et al. (2018) show that incorporating information from inflation expectations—proxied by long-term survey forecasts—can further improve both the estimation of trend inflation and the forecasting performance of univariate UC models. In a related contribution, Banbura, Leiva-Leon, and Menz (2021) augment a small-scale VAR model comprising GDP, inflation, and interest rates with survey-based inflation expectations and demonstrate their relevance for inflation forecasting.

In this paper, we contribute to the aforementioned literature by proposing a new class of large VAR models that incorporates both trend inflation and inflation expectations, proxied by long-term survey forecasts and statistical filters. A key innovation of our approach is its hybrid structure: the model allows for time-varying unconditional means (or trends) in inflation measures while maintaining constant unconditional means for the remaining endogenous variables. Furthermore, we incorporate inflation expectations using the structure proposed by Chan et al. (2018), which enables us to examine whether survey-based

inflation expectations constitute unbiased proxies for model-implied trend inflation. From a computational perspective, we develop an efficient Markov Chain Monte Carlo (MCMC) Gibbs sampler based on the precision matrix algorithms of Chan and Jeliazkov (2009). This approach avoids the computationally intensive Kalman filtering procedures typically used in state-space models.

The proposed specification therefore combines the informational content of a large number (typically $\geqslant 20$) of macroeconomic and financial variables with information from inflation expectations and a time-varying specification of inflation trends. At the same time, the hybrid structure of the model substantially reduces the number of parameters relative to fully time-varying specifications. Together with the proposed efficient sampling algorithm, this feature makes it feasible to conduct computationally demanding recursive forecasting exercises. In the empirical application, we evaluate the proposed framework using a dataset of twenty U.S. macroeconomic variables and an out-of-sample forecasting period spanning the last forty years.

The remainder of the paper is organized as follows. Section 2 presents the model. Section 3 describes the proposed Gibbs sampler. Section 4 reports the estimation results and the out-of-sample forecasting evaluation, while Section 5 concludes.

2 A trend inflation VAR model with inflation expectations

This section introduces a trend-inflation large VAR model augmented with inflation expectations (Ti-VARe) and common stochastic volatility (CSV) in the error terms. The proposed specification has a hybrid structure, as it allows for time-varying unconditional means (or trends) in the inflation measures of interest while maintaining constant unconditional means for the remaining endogenous variables. Although the model can be easily generalized to allow for time variation in the unconditional means of any variable in the system, in this paper we focus exclusively on inflation-related measures.

More formally, the Ti-VARe-CSV model is specified as follows:

$$\boldsymbol{y}_t = \boldsymbol{\tau}_t + \sum_{l=1}^{p} \mathbf{B}_l \left(\boldsymbol{y}_{t-l} - \boldsymbol{\tau}_{t-l}\right) + \boldsymbol{\varepsilon}_t, \qquad \boldsymbol{\varepsilon}_t \sim \mathcal{N}(\mathbf{0}, \exp(h_t)\boldsymbol{\Sigma}) \tag{1}$$

$$\boldsymbol{\tau}_t = \mathbf{S}_\gamma \boldsymbol{\gamma} + \mathbf{S}_{\tau\pi} \boldsymbol{\tau}_t^\pi \tag{2}$$

$$\tau_{j,t}^\pi = \tau_{j,t-1}^\pi + \varepsilon_{j,t}^{\tau\pi}, \quad j = 1, ..., q, \qquad \varepsilon_{j,t}^{\tau\pi} \sim \mathcal{N}(0, \exp(g_{j,t})) \tag{3}$$

$$\pi_{j,t}^e = \alpha_j + \delta_j \tau_{j,t}^\pi + \varepsilon_{j,t}^{\pi e}, \quad j = 1, ..., q, \qquad \varepsilon_{j,t}^{\pi e} \sim \mathcal{N}(0, \varphi_j^2) \tag{4}$$

$$h_t = \rho h_{t-1} + \varepsilon_t^h, \quad |\rho| < 1 \qquad \varepsilon_t^h \sim \mathcal{N}(0, \kappa^2) \tag{5}$$

$$g_{j,t} = g_{j,t-1} + \varepsilon_{j,t}^g, \quad j = 1, .., q \qquad \varepsilon_{j,t}^g \sim \mathcal{N}(0, \lambda_j^2) \tag{6}$$

where $\boldsymbol{y}_t = (y_{1,t}, ..., y_{n,t})'$ is a $n \times 1$ vector of endogenous variables with n potentially large, i.e. $n \geqslant 20$, $\mathbf{B}_1, ..., \mathbf{B}_p$ are $n \times n$ coefficient matrices, $\boldsymbol{\varepsilon}_t$ is an i.i.d. Gaussian error term with common stochastic volatility, i.e. $\exp(h_t)\boldsymbol{\Sigma}$), $\boldsymbol{\Sigma}$ is a $n \times n$ covariance matrix and h_t is the log volatility which follows an AR(1) process described in (5) (see also Chan, 2020a).

Equation (2) defines the unconditional mean of the process, $\mathbb{E}(\boldsymbol{y}_t) = \boldsymbol{\tau}_t$, which consists of a time-invariant component, $\boldsymbol{\gamma}$, and a time-varying component, $\boldsymbol{\tau}_t^\pi$, associated with the

inflation measures. The matrices $\mathbf{S}_\gamma$ and $\mathbf{S}_{\tau\pi}$ are $n\times(n-q)$ and $n\times q$ selection matrices that determine the variables with constant and time-varying unconditional means, respectively. In particular, q denotes the number of variables with evolving trends. The selection matrix $\mathbf{S}_\gamma$ ($\mathbf{S}_{\tau\pi}$) is constructed by selecting the $(n-q)$ (q) columns of the $n\times n$ identity matrix $\mathbf{I}_n$ corresponding to the positions of variables with time-invariant (time-varying) unconditional means.

Example 1 illustrates the structure of the model.

Example 1. *Assume that there are two inflation measures ($q = 2$) ordered second and third in a five-variable ($n = 5$) VAR model. Then, $\mathbf{S}_\gamma$ and $\mathbf{S}_{\tau\pi}$ selection matrices take the form:*

$$\mathbf{S}_\gamma = \begin{bmatrix} 1 & 0 & 0 \\ 0 & 0 & 0 \\ 0 & 0 & 0 \\ 0 & 1 & 0 \\ 0 & 0 & 1 \end{bmatrix} \quad \textit{and} \quad \mathbf{S}_{\tau\pi} = \begin{bmatrix} 0 & 0 \\ 1 & 0 \\ 0 & 1 \\ 0 & 0 \\ 0 & 0 \end{bmatrix}.$$

Next, we model trend inflation, $\tau^\pi_{j,t}$, for $j = 1,\dots,q$, in (3) as a driftless random walk, following the long tradition in time-varying parameter models. In addition, we allow for stochastic volatility in the associated error terms, denoted by $\exp(g_{j,t})$, for $j = 1,\dots,q$. The log-volatility process, $g_{j,t}$, defined in (6), is also assumed to follow a driftless random walk.

Finally, following Chan et al. (2018), we incorporate inflation expectations into the model through an additional measurement equation described in (4). Specifically, inflation expectations, $\pi^e_{j,t}$ for $j = 1,\dots,q$, are assumed to depend on trend inflation. The constant term, α_j, and the slope coefficient, β_j, capture potential biases between the proxy used for inflation expectations and the underlying trend inflation. In the case of an unbiased proxy, inflation expectations would move one-for-one with trend inflation, implying $\beta_j = 1$ and $\alpha_j = 0$.[1]

Overall, the Ti-VARe-CSV model is sufficiently flexible to capture structural changes in trend inflation, incorporate information from inflation expectations, and nest several alternative VAR specifications proposed in the literature. For instance, setting $\mathbf{S}_\gamma = \mathbf{I}_n$ and $\mathbf{S}_{\tau\pi} = \mathbf{0}$ yields a steady-state VAR model (Villani, 2009). Conversely, setting $\mathbf{S}_\gamma = \mathbf{0}$ and $\mathbf{S}_{\tau\pi} = \mathbf{I}_n$, while omitting (4), produces a time-varying steady-state VAR model (D. P. Louzis, 2019). Finally, by imposing $\beta_j = 1$ and $\alpha_j = 0$ we build models similar to those employed in Banbura, Brenna, et al. (2021). Additional details on these restricted specifications of the Ti-VARe-CSV model are provided in Section 4.2.

3 Bayesian estimation

In this section, we present the Markov Chain Monte Carlo (MCMC) algorithm developed to estimate the proposed model. In particular, the Ti-VARe-CSV specification can be formulated as a linear state-space model, which is typically estimated using Kalman filtering techniques (see e.g. D. P. Louzis, 2019; Banbura & van Vlodrop, 2018). However, when

[1]The authors also consider a time-varying parameter specification with MA innovations for (4). Since our focus is primarily on inflation forecasting, we do not adopt this specification, as it would substantially increase the computational burden in recursive forecasting exercises.

the Ti-VARe-CSV model involves a large cross-section of variables (i.e., $n \geqslant 20$), the Kalman filter approach may become computationally burdensome in practice due to the high dimensionality of the state vector.

To address this issue, we rely on the precision-based sampler of Chan and Jeliazkov (2009), which exploits fast band matrix algorithms to efficiently sample high-dimensional state vectors. Using this approach, we develop an efficient estimation algorithm for the Ti-VARe-CSV model and its restricted variants.[2]

3.1 An efficient posterior sampler

Before proceeding to the presentation of the algorithm we first define a number of quantities for both future reference and notational convenience. To that end, we stack $\boldsymbol{y}_t$ over t and we define $\boldsymbol{y} = (\boldsymbol{y}_1', ..., \boldsymbol{y}_T')'$, while the quantities $\boldsymbol{\tau}^{\pi}$, $\boldsymbol{\pi}^{e}$, $\boldsymbol{\varepsilon}$, $\boldsymbol{\varepsilon}^{\pi e}$, $\boldsymbol{\varepsilon}^{h}$, $\boldsymbol{\varepsilon}^{g}$ are defined similarly. The vectors $\boldsymbol{h}$ and $\boldsymbol{g}_j$ $\forall j$ gather the stochastic volatility of the error terms and are defined as $\boldsymbol{h} = (\boldsymbol{h}_1, ..., \boldsymbol{h}_T)'$ and $\boldsymbol{g}_j = (\boldsymbol{g}_{j1}, ..., \boldsymbol{g}_{jT})'$.[3]

We sequentially draw the Ti-VARe-CSV coefficients from their respective conditional posterior densities using the following Gibbs sampler:

1. $p(\boldsymbol{\tau}^{\pi}|\boldsymbol{y}, \boldsymbol{\pi}^{e}, \mathbf{B}, \boldsymbol{\Sigma}, \boldsymbol{h}, \boldsymbol{\gamma}, \boldsymbol{\tau}_0^{\pi}, \{\boldsymbol{g}_j\}_{j=1}^{q})$;
2. $p(\boldsymbol{\gamma}|\boldsymbol{y}, \boldsymbol{\pi}^{e}, \mathbf{B}, \boldsymbol{\Sigma}, \boldsymbol{h}, \boldsymbol{\tau}^{\pi})$;
3. $p(\mathbf{B}, \boldsymbol{\Sigma}|\boldsymbol{y}, \boldsymbol{\pi}^{e}, \boldsymbol{\gamma}, \boldsymbol{\tau}^{\pi}, \boldsymbol{h})$;
4. $p(\boldsymbol{h}|\boldsymbol{y}, \boldsymbol{\pi}^{e}, \mathbf{B}, \boldsymbol{\Sigma}, \boldsymbol{\gamma}, \boldsymbol{\tau}^{\pi})$;
5. $p(\boldsymbol{g}_j|\boldsymbol{y}, \boldsymbol{\pi}^{e}, \boldsymbol{\tau}^{\pi}, g_{j0}, \lambda_j^2)$ for $j = 1, ..., q$;
6. $p(\boldsymbol{\tau}_0^{\pi}|\boldsymbol{y}, \boldsymbol{\pi}^{e}, \boldsymbol{\tau}_1^{\pi}, \{\boldsymbol{g}_j\}_{j=1}^{q}))$;
7. $p(\boldsymbol{\vartheta}|\boldsymbol{y}, \boldsymbol{\pi}^{e}, \boldsymbol{\tau}^{\pi}, \boldsymbol{\gamma}, \mathbf{B}, \boldsymbol{\Sigma}, \boldsymbol{h}, \{\boldsymbol{g}_j\}_{j=1}^{q},)$;

where $\boldsymbol{\vartheta} = (\kappa^2, \rho, \{\alpha_j, \delta_j, \varphi_j^2, g_{j,0}, \lambda_j^2\}_{j=1}^{q})$, $\mathbf{B} = (\mathbf{B}_1, ..., \mathbf{B}_n)'$ and $\boldsymbol{\tau}_0^{\pi}$ and $g_{j,0}$ are the starting values for $\boldsymbol{\tau}^{\pi}$ and $\boldsymbol{g}_{j,0}$, respectively, which are treated as unknown parameters.

Next, we discuss how to sample efficiently from the posterior densities concentrating on steps 1 and 2, since the residual steps are standard in the literature and the interested reader is referred to (Chan, 2020b). Especially, sampling $\boldsymbol{\tau}^{\pi}$ is of great interest in computational terms since it is the most time consuming step of the algorithm.

In order to implement **Step 1** we should first notice that $\boldsymbol{\tau}^{\pi}$ is employed in measurement equations (1) and (4) and also in state equation (3). Therefore, we should use all three sources of information to derive the posterior density of $\boldsymbol{\tau}^{\pi}$ given that innovations, $\boldsymbol{\varepsilon}_t$, $\boldsymbol{\varepsilon}_t^{\tau\pi}$, $\boldsymbol{\varepsilon}_t^{\pi e}$ are i.i.d and independent from each other. Next, we derive expressions in matrix notation for each of the equations which enable us to implement the precision matrix algorithm.

[2] See Joshua Chan's webpage (`https://joshuachan.org/`) for various applications of the precision sampler.

[3] $\boldsymbol{y}$ and $\boldsymbol{\varepsilon}$ are $nT \times 1$, $\boldsymbol{\pi}^{e}$, $\boldsymbol{\tau}^{\pi}$, $\boldsymbol{\varepsilon}^{\tau\pi}$ and $\boldsymbol{\varepsilon}^{\pi e}$ are $qT \times 1$, $\boldsymbol{h}$ and $\boldsymbol{g}_j$ are $T \times 1$ vectors.

In particular, we can rewrite (1) as (see Appendix B.1 for more details):

$$\tilde{\boldsymbol{y}}_\gamma = \mathbf{H}_B \bar{\mathbf{S}}_{\tau\pi} \boldsymbol{\tau}^\pi + \boldsymbol{\varepsilon}, \qquad \boldsymbol{\varepsilon} \sim \mathcal{N}(\mathbf{0}, \boldsymbol{\Omega} \otimes \boldsymbol{\Sigma}) \tag{7}$$

where $\tilde{\boldsymbol{y}}_\gamma = \mathbf{H}_B \bar{\boldsymbol{y}}_\gamma$, $\bar{\boldsymbol{y}}_\gamma = \boldsymbol{y} - \bar{\mathbf{S}}_\gamma \boldsymbol{\gamma}$, $\bar{\mathbf{S}}_\gamma = \mathbf{1}_T \otimes \mathbf{S}_\gamma$, $\bar{\mathbf{S}}_{\tau\pi} = \mathbf{I}_T \otimes \mathbf{S}_{\tau\pi}$, $\boldsymbol{\Omega} = \text{diag}(\exp(h_1), ..., \exp(h_T))$ and $\mathbf{H_B}$ is the following square $(nT \times nT)$ band matrix:

$$\mathbf{H_B} = \begin{bmatrix} \mathbf{I}_n & \mathbf{0} & \mathbf{0} & \dots & \mathbf{0} \\ -\mathbf{B}_1 & \mathbf{I}_n & \mathbf{0} & \dots & \mathbf{0} \\ -\mathbf{B}_2 & -\mathbf{B}_1 & \mathbf{I}_n & \dots & \mathbf{0} \\ \vdots & \ddots & \ddots & \ddots & \mathbf{0} \\ \mathbf{0} & -\mathbf{B}_p & \dots & -\mathbf{B}_1 & \mathbf{I}_n \end{bmatrix} \tag{8}$$

Therefore, by a simple change of variable we can write $\tilde{\boldsymbol{y}}_\gamma | \mathbf{B}, \boldsymbol{\Sigma}, \boldsymbol{\Omega}, \boldsymbol{\tau}^\pi, \boldsymbol{\gamma} \sim \mathcal{N}(\mathbf{H}_B \bar{\mathbf{S}}_{\tau\pi} \boldsymbol{\tau}^\pi, \boldsymbol{\Omega} \otimes \boldsymbol{\Sigma})$ implying the following log density:

$$\log p(\tilde{\boldsymbol{y}}_\gamma | \mathbf{B}, \boldsymbol{\Sigma}, \boldsymbol{h}, \boldsymbol{\tau}^\pi, \boldsymbol{\gamma}) \propto -\frac{1}{2} (\tilde{\boldsymbol{y}}_\gamma - \mathbf{H}_B \bar{\mathbf{S}}_{\tau\pi} \boldsymbol{\tau}^\pi)' (\boldsymbol{\Omega}^{-1} \otimes \boldsymbol{\Sigma}^{-1}) (\tilde{\boldsymbol{y}}_\gamma - \mathbf{H}_B \bar{\mathbf{S}}_{\tau\pi} \boldsymbol{\tau}^\pi) \tag{9}$$

where $\boldsymbol{\Omega}^{-1} = \text{diag}(\exp(-h_1), ..., \exp(-h_T))$.

Next we rewrite (4) as:

$$\tilde{\boldsymbol{\pi}}^e = \mathbf{D} \boldsymbol{\tau}^\pi + \boldsymbol{\varepsilon}^{\pi e}, \qquad \boldsymbol{\varepsilon}^{\pi e} \sim \mathcal{N}(\mathbf{0}, \mathbf{I}_T \otimes \boldsymbol{\Phi}) \tag{10}$$

where $\tilde{\boldsymbol{\pi}}^e = \boldsymbol{\pi}^e - \boldsymbol{\alpha}$, $\boldsymbol{\alpha} = \mathbf{1}_T \otimes (\alpha_1, ..., \alpha_q)'$, $\mathbf{D} = \mathbf{I}_T \otimes (\delta_1, ..., \delta_q)'$ and $\boldsymbol{\Phi} = \text{diag}(\varphi_1^2, ..., \varphi_q^2)$ with joint conditional distribution $\tilde{\boldsymbol{\pi}}^e | \boldsymbol{\alpha}, \mathbf{D}, \boldsymbol{\tau}^\pi, \boldsymbol{\Phi} \sim \mathcal{N}(\mathbf{D} \boldsymbol{\tau}^\pi, \mathbf{I}_T \otimes \boldsymbol{\Phi})$ and log density:

$$\log p(\tilde{\boldsymbol{\pi}}^e | \boldsymbol{\tau}^\pi, \boldsymbol{\alpha}, \mathbf{D}, \boldsymbol{\Phi}) \propto -\frac{1}{2} (\tilde{\boldsymbol{\pi}}^e - \mathbf{D} \boldsymbol{\tau}^\pi)' (\mathbf{I}_T \otimes \boldsymbol{\Phi}^{-1}) (\tilde{\boldsymbol{\pi}}^e - \mathbf{D} \boldsymbol{\tau}^\pi) \tag{11}$$

Thus far, we have re-framed measurement equations (1) and (4) as normal linear regressions and we can derive their log likelihood by just adding the log densities in (9) and (11). Now, we need a prior distribution for $\boldsymbol{\tau}^\pi$ so as to derive its conditional posterior distribution via the Bayes rule. Hence, we rewrite the state equation in(3) as:

$$\mathbf{H} \boldsymbol{\tau}^\pi = \mathbf{a}_{\tau\pi} + \boldsymbol{\epsilon}^{\tau\pi}, \qquad \boldsymbol{\epsilon}^{\tau\pi} \sim \mathcal{N}(\mathbf{0}, \mathbf{G}) \tag{12}$$

where $\mathbf{a}_{\tau\pi} = (\boldsymbol{\tau}_0^{\pi\prime}, \mathbf{0}, ..., \mathbf{0})'$ with $\boldsymbol{\tau}_0^\pi$ being a $q \times 1$ vector of the starting values of the process, $\mathbf{G} = \text{diag}((\exp(g_{1,1}), ..., \exp(g_{q,1}))', ..., (\exp(g_{1,T}), ..., \exp(g_{q,T}))')$ and $\mathbf{H}$ is a $qT \times qT$ matrix defined as:

$$\mathbf{H} = \begin{bmatrix} \mathbf{I}_q & \mathbf{0} & \mathbf{0} & \dots & \mathbf{0} \\ -\mathbf{I}_q & \mathbf{I}_q & \mathbf{0} & \dots & \mathbf{0} \\ \mathbf{0} & -\mathbf{I}_q & \mathbf{I}_q & \dots & \mathbf{0} \\ \vdots & \ddots & \ddots & \ddots & \mathbf{0} \\ \mathbf{0} & \mathbf{0} & \dots & -\mathbf{I}_q & \mathbf{I}_q \end{bmatrix} \tag{13}$$

At this point we should note that both $\mathbf{H_B}$ and $\mathbf{H}$ are sparse matrices, i.e. the vast majority of entries are zero, where the non-zero elements are arranged below the main unitary diagonal. This structure leads to significant computational gains and since it holds

that $|\mathbf{H_B}| = |\mathbf{H}| = 1\ \forall \mathbf{B}_i$, the matrices are invertible meaning that we can rephrase (12) as (Chan & Jeliazkov, 2009; Chan, 2013):[4,5]

$$\boldsymbol{\tau}^{\pi} = \tilde{\boldsymbol{\tau}}^{\pi} + \tilde{\boldsymbol{\epsilon}}^{\tau\pi}, \qquad \tilde{\boldsymbol{\epsilon}}^{\tau\pi} \sim \mathcal{N}(\mathbf{0}, \tilde{\mathbf{G}}) \tag{14}$$

where $\tilde{\boldsymbol{\tau}}^{\pi} = \mathbf{H}^{-1}\mathbf{a}_{\tau\pi} = \mathbf{1}_T \otimes \boldsymbol{\tau}_0^{\pi}$, $\tilde{\boldsymbol{\epsilon}}^{\tau\pi} = \mathbf{H}^{-1}\boldsymbol{\epsilon}^{\tau\pi}$ and $\tilde{\mathbf{G}} = (\mathbf{H}'\mathbf{G}^{-1}\mathbf{H})^{-1}$, implying a Gaussian prior distribution for $\boldsymbol{\tau}^{\pi}$, i.e. $\boldsymbol{\tau}^{\pi}|\boldsymbol{\tau}_0^{\pi}, \mathbf{G} \sim \mathcal{N}(\tilde{\boldsymbol{\tau}}^{\pi}, \tilde{\mathbf{G}})$ with log density:

$$\log p(\boldsymbol{\tau}^{\pi}|\boldsymbol{\tau}_0^{\pi}, \mathbf{G}) \propto -\frac{1}{2}(\boldsymbol{\tau}^{\pi} - \tilde{\boldsymbol{\tau}}^{\pi})'\tilde{\mathbf{G}}^{-1}(\boldsymbol{\tau}^{\pi} - \tilde{\boldsymbol{\tau}}^{\pi}) \tag{15}$$

Now, we can derive the conditional posterior distribution for $\boldsymbol{\tau}^{\pi}$ by combining the likelihood, (9) and (11), with the prior, (15). We ignore any term not including $\boldsymbol{\tau}^{\pi}$ and we apply the *completing-the-squares* technique to get:

$$\begin{aligned}
\log p(\boldsymbol{\tau}^{\pi}|\boldsymbol{y}, \boldsymbol{\pi}^{e}, \mathbf{B}, \boldsymbol{\Sigma}, \boldsymbol{h}, \boldsymbol{\gamma}, \boldsymbol{\tau}_0^{\pi}, \{\boldsymbol{g}_j\}_{j=1}^{q}) \propto & -\frac{1}{2}(\tilde{\boldsymbol{y}}_{\gamma} - \mathbf{H}_B\bar{\mathbf{S}}_{\tau\pi}\boldsymbol{\tau}^{\pi})'(\boldsymbol{\Omega}^{-1} \otimes \boldsymbol{\Sigma}^{-1})(\tilde{\boldsymbol{y}}_{\gamma} - \mathbf{H}_B\bar{\mathbf{S}}_{\tau\pi}\boldsymbol{\tau}^{\pi}) \\
& -\frac{1}{2}(\boldsymbol{\pi}^{e} - \boldsymbol{\alpha} - \mathbf{D}\boldsymbol{\tau}^{\pi})'(\mathbf{I}_T \otimes \boldsymbol{\Phi}^{-1})(\boldsymbol{\pi}^{e} - \boldsymbol{\alpha} - \mathbf{D}\boldsymbol{\tau}^{\pi}) \\
& -\frac{1}{2}(\boldsymbol{\tau}^{\pi} - \tilde{\boldsymbol{\tau}}^{\pi})'\tilde{\mathbf{G}}^{-1}(\boldsymbol{\tau}^{\pi} - \tilde{\boldsymbol{\tau}}^{\pi}) \\
\propto & -\frac{1}{2}\Big\{-2\boldsymbol{\tau}^{\pi\prime}\Big[\bar{\mathbf{S}}'_{\tau\pi}\mathbf{H}'_B(\boldsymbol{\Omega}^{-1} \otimes \boldsymbol{\Sigma}^{-1})\tilde{\boldsymbol{y}}_{\gamma} \dots \\
& +\mathbf{D}'(\mathbf{I}_T \otimes \boldsymbol{\Phi}^{-1})(\boldsymbol{\pi}^{e} - \boldsymbol{\alpha}) + \tilde{\mathbf{G}}^{-1}\tilde{\boldsymbol{\tau}}^{\pi}\Big] \dots \\
& +\boldsymbol{\tau}^{\pi\prime}\Big[\bar{\mathbf{S}}'_{\tau\pi}\mathbf{H}'_B(\boldsymbol{\Omega}^{-1} \otimes \boldsymbol{\Sigma}^{-1})\mathbf{H}_B\bar{\mathbf{S}}_{\tau\pi} + \mathbf{D}'(\mathbf{I}_T \otimes \boldsymbol{\Phi}^{-1})\mathbf{D} + \tilde{\mathbf{G}}^{-1}\Big]\boldsymbol{\tau}^{\pi}\Big\} \\
\propto & -\frac{1}{2}\left(-2\boldsymbol{\tau}^{\pi\prime}\mathbf{K}_{\tau\pi}^{-1}\hat{\boldsymbol{\tau}}^{\pi} + \boldsymbol{\tau}^{\pi\prime}\mathbf{K}_{\tau\pi}^{-1}\boldsymbol{\tau}^{\pi} + \hat{\boldsymbol{\tau}}^{\pi\prime}\mathbf{K}_{\tau\pi}^{-1}\hat{\boldsymbol{\tau}}^{\pi}\right) \\
\propto & -\frac{1}{2}(\boldsymbol{\tau}^{\pi} - \hat{\boldsymbol{\tau}}^{\pi})'\mathbf{K}_{\tau\pi}^{-1}(\boldsymbol{\tau}^{\pi} - \hat{\boldsymbol{\tau}}^{\pi})
\end{aligned} \tag{16}$$

which is a multivariate Gaussian kernel with mean $\hat{\boldsymbol{\tau}}^{\pi}$ and covariance matrix $\mathbf{K}_{\tau\pi}$, implying a Gaussian conditional posterior distribution for $\boldsymbol{\tau}^{\pi}$ of the form:

$$\boldsymbol{\tau}^{\pi}|\boldsymbol{y}, \boldsymbol{\pi}^{e}, \mathbf{B}, \boldsymbol{\Sigma}, \boldsymbol{h}, \boldsymbol{\gamma}, \boldsymbol{\tau}_0^{\pi}, \{\boldsymbol{g}_j\}_{j=1}^{q} \sim \mathcal{N}(\hat{\boldsymbol{\tau}}^{\pi}, \mathbf{K}_{\tau\pi}) \tag{17}$$

where $\mathbf{K}_{\tau\pi} = [(\mathbf{H}_B\bar{\mathbf{S}}_{\tau\pi})'(\boldsymbol{\Omega}^{-1} \otimes \boldsymbol{\Sigma}^{-1})(\mathbf{H}_B\bar{\mathbf{S}}_{\tau\pi}) + \mathbf{D}'(\mathbf{I}_T \otimes \boldsymbol{\Sigma}_{\pi e}^{-1})\mathbf{D} + \tilde{\mathbf{G}}^{-1}]^{-1}$ and $\hat{\boldsymbol{\tau}}^{\pi} = \mathbf{K}_{\tau\pi}^{-1}[(\mathbf{H}_B\bar{\mathbf{S}}_{\tau\pi})'(\boldsymbol{\Omega}^{-1} \otimes \boldsymbol{\Sigma}^{-1})\tilde{\boldsymbol{y}}_{\gamma} + \mathbf{D}'(\mathbf{I}_T \otimes \boldsymbol{\Sigma}_{\pi e}^{-1})(\boldsymbol{\pi}^{e} - \boldsymbol{\alpha}) + \tilde{\mathbf{G}}^{-1}\tilde{\boldsymbol{\tau}}^{\pi}]$.

Turning to **Step 2**, we work similarly and we rewrite (1) as a standard linear regression using matrix notation:

$$\tilde{\boldsymbol{y}}_{\tau\pi} = \mathbf{H}_B\bar{\mathbf{S}}_{\gamma}\boldsymbol{\gamma} + \boldsymbol{\varepsilon}, \qquad \boldsymbol{\varepsilon} \sim \mathcal{N}(\mathbf{0}, \boldsymbol{\Omega} \otimes \boldsymbol{\Sigma}) \tag{18}$$

[4] $|.|$ denotes the determinant. See also (Chan, 2017) for a textbook treatment of fast band matrix algorithm methods.

[5] First, it is trivial to show that $\tilde{\boldsymbol{\Sigma}} = Cov(\tilde{\boldsymbol{\varepsilon}}) = Cov(\mathbf{H_B}^{-1}\boldsymbol{\varepsilon}) = \mathbf{H_B}^{-1}Cov(\boldsymbol{\varepsilon})\mathbf{H_B}^{-1\prime} = \mathbf{H_B}^{-1}(\mathbf{I}_T \otimes \boldsymbol{\Sigma})\mathbf{H_B}^{-1\prime}$ using standard covariance properties. Second, for computational efficiency reasons it is often more convenient to write $\tilde{\boldsymbol{\Sigma}} = (\tilde{\boldsymbol{\Sigma}}^{-1})^{-1} = (\mathbf{H_B}'(\mathbf{I}_T \otimes \boldsymbol{\Sigma}^{-1})\mathbf{H_B})^{-1}$. This last result follows from the fact that for any three invertible square matrices holds that $(\mathbf{ABC})^{-1} = \mathbf{C}^{-1}\mathbf{B}^{-1}\mathbf{A}^{-1}$ and also that $(\mathbf{I}_T \otimes \boldsymbol{\Sigma})^{-1} = \mathbf{I}_T \otimes \boldsymbol{\Sigma}^{-1}$.

where $\tilde{\boldsymbol{y}}_{\tau\pi} = \mathbf{H}_B\bar{\boldsymbol{y}}_{\tau\pi}$ and $\bar{\boldsymbol{y}}_{\tau\pi} = \boldsymbol{y} - \bar{\mathbf{S}}_{\tau\pi}\boldsymbol{\tau}^{\pi}$ with conditional distribution $\tilde{\boldsymbol{y}}_{\tau\pi}|\mathbf{B}, \boldsymbol{\Sigma}, \boldsymbol{h}, \boldsymbol{\tau}^{\pi}, \boldsymbol{\gamma} \sim \mathcal{N}(\mathbf{H}_B\bar{\mathbf{S}}_{\gamma}\boldsymbol{\gamma}, \boldsymbol{\Omega} \otimes \boldsymbol{\Sigma})$ and log density:

$$\log p(\tilde{\boldsymbol{y}}_{\tau\pi}|\mathbf{B}, \boldsymbol{\Sigma}, \boldsymbol{h}, \boldsymbol{\tau}^{\pi}, \boldsymbol{\gamma}) \propto -\frac{1}{2}(\tilde{\boldsymbol{y}}_{\mu} - \mathbf{H}_B\bar{\mathbf{S}}_{\gamma}\boldsymbol{\gamma})'(\boldsymbol{\Omega}^{-1} \otimes \boldsymbol{\Sigma}^{-1})(\tilde{\boldsymbol{y}}_{\mu} - \mathbf{H}_B\bar{\mathbf{S}}_{\gamma}\boldsymbol{\gamma}) \tag{19}$$

Assuming a Gaussian prior distribution for $\boldsymbol{\gamma}$, i.e. $\boldsymbol{\gamma} \sim \mathcal{N}(\boldsymbol{\gamma}_0, \mathbf{V}_{\gamma})$, and applying standard regression results, we can show that the posterior distribution of $\boldsymbol{\gamma}$ is given by:

$$\boldsymbol{\gamma}|\boldsymbol{y}, \mathbf{B}, \boldsymbol{\Sigma}, \boldsymbol{h}, \boldsymbol{\tau}^{\pi} \sim \mathcal{N}(\hat{\boldsymbol{\gamma}}, \mathbf{K}_{\gamma}) \tag{20}$$

where $\mathbf{K}_{\gamma} = [(\mathbf{H}_B\bar{\mathbf{S}}_{\gamma})'(\boldsymbol{\Omega}^{-1} \otimes \boldsymbol{\Sigma}^{-1})(\mathbf{H}_B\bar{\mathbf{S}}_{\gamma}) + \mathbf{V}_{\gamma}^{-1}]^{-1}$ and $\hat{\boldsymbol{\gamma}} = \mathbf{K}_{\gamma}^{-1}[(\mathbf{H}_B\bar{\mathbf{S}}_{\gamma})'(\boldsymbol{\Omega}^{-1} \otimes \boldsymbol{\Sigma}^{-1})\tilde{\boldsymbol{y}}_{\tau\pi} + \mathbf{V}_{\gamma}^{-1}\boldsymbol{\gamma}_0]$.

3.1.1 Improving the efficiency of the algorithm

We can further improve the computational efficiency of the algorithm if we elaborate more on specific quantities of the algorithm. In particular, we focus on the computation of products which contain the sparse matrix $\mathbf{H}_B$ and are of crucial importance in terms of numerical efficiency of the algorithm.

More specifically, in Propositions C.1 and C.2 (see the Technical Appendix C) we show that $\mathbf{H}_B\bar{\mathbf{S}}_{\tau\pi}$ and $\mathbf{H}_B\bar{\mathbf{S}}_{\gamma}$ in (7) and (18), respectively, can be alternatively computed much more efficiently relying only on p matrix multiplications, i.e. $\{\mathbf{B}_i\mathbf{S}_{\tau\pi}\}_{i=1}^{p}$ and $\{\mathbf{B}_i\mathbf{S}_{\gamma}\}_{i=1}^{p}$. In even more detail, computing $\mathbf{H}_B\bar{\mathbf{S}}_{\tau\pi}$ or $\mathbf{H}_B\bar{\mathbf{S}}_{\gamma}$ requires $\mathcal{O}q\{np[T-1-(p-1)/2]+T\})$ arithmetic operations while the alternative method has a complexity of order $\mathcal{O}(pnq)$. For $T > (p+3)/2$, which is always true in a typical macroeconometric application with a standard data and lag length, e.g. $T \geqslant 40$ and $p \in [2, 13]$, we show that $\mathcal{O}(pnq) < \mathcal{O}(q\{np[T-1-(p-1)/2]+T\})$, implying that for larger samples, i.e. as $T \to \infty$, we obtain greater computational gains.

The sparse matrix $\mathbf{H}_B$ is also involved in the calculation of $\tilde{\boldsymbol{y}}_{\gamma} = \mathbf{H}_B\bar{\boldsymbol{y}}_{\gamma}$ in (7) which, as we show in Proposition C.3, is $\mathcal{O}(n\{np[T-1-(p-1)/2]+T\})$; however, we can alternatively compute $\tilde{\boldsymbol{y}}_{\gamma}$ in a computationally efficient way as $\tilde{\boldsymbol{y}}_{\gamma} = (\tilde{\boldsymbol{y}}'_{\gamma 1}, ..., \tilde{\boldsymbol{y}}'_{\gamma T})'$ where $\tilde{\boldsymbol{y}}_{\gamma t} = \bar{\boldsymbol{y}}_{\gamma,t} - \mathbf{B}_1\bar{\boldsymbol{y}}_{\gamma,t-1} - ... - \mathbf{B}_p\bar{\boldsymbol{y}}_{\gamma,t-p}$ and $\bar{\boldsymbol{y}}_{\gamma,t} = \boldsymbol{y}_t - \mathbf{S}_{\tau\pi}\tau_t^{\pi}$. The latter approach requires $\mathcal{O}(n^2p[T-(p+1)/2])$ arithmetic operations which is always smaller than the arithmetic operations required to compute $\mathbf{H}_B\bar{\boldsymbol{y}}_{\gamma}$ (see Proposition C.3) proving the efficiency of the alternative method over the sparse matrix multiplication. The same result also holds for $\tilde{\boldsymbol{y}}_{\tau\pi} = \mathbf{H}_B\bar{\boldsymbol{y}}_{\tau\pi}$ in (18), which can also be calculated more efficiently by constructing the vector $\tilde{\boldsymbol{y}}_{\tau\pi} = (\tilde{\boldsymbol{y}}'_{\tau\pi,1}, ..., \tilde{\boldsymbol{y}}'_{\tau\pi,T})'$ where $\tilde{\boldsymbol{y}}_{\tau\pi,t} = \bar{\boldsymbol{y}}_{\tau\pi,t} - \mathbf{B}_1\bar{\boldsymbol{y}}_{\tau\pi,t-1} - ... - \mathbf{B}_p\bar{\boldsymbol{y}}_{\tau\pi,t-p}$ and $\bar{\boldsymbol{y}}_{\tau\pi,t} = \boldsymbol{y}_t - \mathbf{S}_{\gamma}\gamma$.[6]

4 Empirical work

4.1 Data and inflation expectation proxies

The empirical analysis of the proposed model is based on a dataset of twenty quarterly macroeconomic and financial variables from the U.S. economy, covering more than sixty

[6]To be precise, the two methods are equivalent if we assume $\boldsymbol{y}_0 = \boldsymbol{y}_{-1} =, ..., = \boldsymbol{y}_{1-p} = 0$

years, from 1959Q2 to 2021Q3. The selection of variables follows the recent large VAR literature (see e.g. Chan, 2022, for a recent contribution) and the data are obtained from the FRED-QD database maintained by the Federal Reserve Bank of St. Louis (McCracken & Ng, 2020). The dataset includes standard measures of economic activity, inflation, labor market conditions, money supply, interest rates, and other financial indicators. Most variables are transformed into annualized growth rates to achieve stationarity, with the exception of the unemployment rate and interest rates. A detailed description of all variables and their corresponding transformations is provided in Appendix A.

In the remainder of the paper, we focus on three measures of inflation, $\pi_{j,t}$, which are widely used in both academic research and monetary policy analysis by the Federal Reserve: Consumer Price Index (CPI) inflation, Personal Consumption Expenditures (PCE) inflation, and the GDP price deflator (GDPd).[7] As noted by Chan et al. (2018), CPI inflation is easily communicated to the public; however, its historical data do not fully reflect methodological changes, which may introduce structural instabilities. In contrast, PCE inflation is regularly revised to account for methodological changes and is the reference measure for the Federal Reserve's long-run inflation target. We also report results for the GDP deflator, as it is typically included in large VAR datasets and therefore provides a useful benchmark for assessing the forecasting performance of the proposed framework.

Following the recent literature, and subject to data availability, we employ survey-based long-term inflation forecasts as well as exponential weighted moving average (EWMA) filters to proxy inflation expectations for each of the three inflation measures, denoted by $\pi^e_{j,t}$ for $j \in \text{CPI}, \text{PCE}, \text{GDPd}$ (see e.g. Chan et al., 2018; Bańbura & Bobeica, 2022).[8] Table 1 summarizes the proxies used to construct the inflation expectations series.

More specifically, CPI inflation expectations are proxied using long-term forecasts from the Blue Chip Consensus and the Survey of Professional Forecasters (SPF) conducted by the Federal Reserve Bank of Philadelphia. For the period 1959Q2–1979Q4, during which survey-based expectations are unavailable, we use the EWMA filter to construct the corresponding expectations series. For PCE inflation, we employ the long-run PCE inflation expectation series (PTR) from the Federal Reserve Board's FRB/US econometric model, and missing observations for 1959Q2–1967Q4 are imputed using the EWMA filter.[9] Finally, for the GDP deflator, we rely exclusively on the EWMA filter to proxy long-run inflation expectations, since no publicly available survey-based forecasts exist for this measure.

[7] The corresponding mnemonics in the FRED-QD database are CPIAUCSL, PCECTPI, and GDPCTPI.

[8] The exponential weighted moving average (EWMA) filter has been widely used as a proxy for trend inflation in U.S. inflation forecasting studies (see e.g. Clark & McCracken, 2011; Faust & Wright, 2013; Clark & McCracken, 2010) as well as in studies for the euro area (Bańbura & Bobeica, 2022).

[9] PTR is a quasi survey-based measure, as part of the series is constructed using an econometric component; see Chan et al. (2018) for details.

Table 1: Proxies used as inflation expectations

	Periods[1]			
Inflation measures	1959 Q2 - 1967 Q4	1967 Q1 - 1979 Q4	1980 Q1 - 1991 Q3	1991 Q4 - 2021 Q3
CPI inflation	EWMA[2]		Blue Chip[3]	Philadelphia[4]
PCE inflation	EWMA	PTR[5]		
GDP deflator	EWMA			

[1] The cells of the inflation expectation proxies used for more than one period are colored in light blue.
[2] EWMA is $\pi_{j,t}^{eEWMA} = \lambda \pi_{j,t-1}^{eEWMA} + (1-\lambda)\pi_{j,t-1}$ with $\lambda = 0.96$ and $j = CPI, PCE, GDP$.
[3] Blue Chip are the survey based long-term (6-10 years) inflation forecasts taken twice a year (March and October) from Blue Chip Economic Indicators and are obtain from the Federal Reserve Bank of Philadelphia, https://www.philadelphiafed.org/surveys-and-data/real-time-data-research/inflation-forecasts. We use linear interpolation for the missing observations.
[4] Philadelphia denotes the 10-year-ahead inflation forecats from the survey of professional forecasters of the Federal Reserve Bank of Philadelphia, https://www.philadelphiafed.org/surveys-and-data/real-time-data-research/inflation-forecasts.
[5] PTR denotes the long-run PCE inflation expectation series included in the Federal Reserve Board of Governor's FRB/US econometric model and is taken from https://www.federalreserve.gov/econres/us-models-package.htm.

We argue that using a statistical filter to proxy inflation expectations in the absence of publicly available data is the preferred approach for two main reasons. First, the empirical literature shows that detrending inflation measures with an EWMA filter enhances the forecasting performance of models, at least for the U.S. economy (Clark & McCracken, 2011; Faust & Wright, 2013; Clark & McCracken, 2010) (see also Banbura, Leiva-Leon, and Menz (2021) for the euro area). These findings suggest that the EWMA filter contains valuable information that can be incorporated into the model, particularly in the measurement equation (4). Second, a visual comparison of the EWMA-based and survey-based inflation expectations indicates that the two series are remarkably similar over the entire sample period.

The long span of the data set allows us to assess the model's performance across all major periods of recent U.S. economic history, including the Great Inflation of the 1970s and early 1980s, the subsequent Great Moderation, and the Global Financial Crisis of 2007–2009. The post-COVID-19 inflation episode is also included, enabling an evaluation of the model's forecasting ability during the current high-inflation environment.

4.2 Competing models

Table 2 summarizes the alternative models considered in this study, while additional details are provided in Appendix D. In particular, we estimate several restricted versions of the proposed Ti-VARe-CSV model in order to investigate a range of research questions related to inflation forecasting and trend inflation estimation within a large VAR framework.

Table 2: Alternative (restricted) specifications

Name	Brief description
M0	VAR-CSV (Chan, 2020a).
M1	The proposed model with $\mathbf{S}_\gamma = \mathbf{I}_n$ and $\mathbf{S}_{\tau\pi} = \mathbf{0}$ resulting in a steady-state VAR-CSV (D. P. Louzis, 2019).
M2	The proposed model without the inflation expectation equation (4) and an extra common trend inflation factor.
M3	The M2 model without the common trend inflation factor.
M4	Restricts the proposed model so that $\alpha_j = 0$, $\delta_j = 1$ and $g_{j,t} \forall j$ is constant; we use the EWMA filter to proxy inflation expectations.
M5	The M4 model but with the inflation expectation proxies of Table 1.
M6	The M5 model with stochastic volatility in the error terms of the trend inflation equation 3.
M7	The proposed model Ti-VARe-CSV.

For instance, by setting $\mathbf{S}\gamma = \mathbf{I}_n$ and $\mathbf{S}_{\tau\pi} = \mathbf{0}$ in the proposed model (M7), we obtain model M1, which corresponds to a large steady-state VAR-CSV specification proposed by D. P. Louzis (2019). This specification allows us to investigate whether imposing an informative prior on the unconditional mean of the process can materially improve inflation forecasting relative to the benchmark VAR-CSV model of Chan (2020a), which serves as our baseline model (M0).[10]

Models M2 and M3 are also restricted versions of the proposed M7 specification, as they do not incorporate information from inflation expectations. Nevertheless, these models allow us to examine the extent of time variation in trend inflation and to assess whether such variation improves inflation forecasting accuracy.

The remaining restricted specifications—models M4, M5, and M6—incorporate inflation expectations through the measurement equation (4), as in the proposed model. However, following Chan et al. (2018), we impose additional restrictions on (4) in order to investigate whether specific features of the inflation expectations specification improve trend inflation estimation and inflation predictability.

More specifically, models M4 and M5 assume that the selected measure of inflation expectations is an unbiased proxy for trend inflation. This restriction implies $\alpha_j = 0$ and $\delta_j = 1$ for all j, as in Banbura, Leiva-Leon, and Menz (2021). In addition, these models assume homoscedastic error terms in (4), implying that $g_{j,t}$ is constant for all j. The difference between M4 and M5 lies in the proxy used for inflation expectations. Model M4 uses the EWMA statistical filter for all inflation measures, whereas model M5 employs survey-based long-term inflation forecasts whenever such data are available. This comparison allows us to assess whether survey-based proxies for inflation expectations contain additional useful information for forecasting relative to a backward-looking statistical filter. Finally, model M6 is similar to M5 but relaxes the homoscedasticity assumption by allowing the volatility process $g_{j,t}$ to vary over time.

[10]The authors in Chan (2020a, 2020b) repeatedly demonstrate the superior forecasting performance of large-scale VAR-CSV models relative to small-n systems or specifications with constant volatility using a similar dataset. Therefore, including a Ti-VARe specification with a small cross-section or without common stochastic volatility would be of limited empirical interest for this study. Our framework could also be extended to account for MA and fat-tailed innovations, as proposed by Chan (2020a), but this extension is beyond the scope of the present paper. For a related discussion see D. P. Louzis (2019).

4.3 In-sample estimation results

This section presents the estimation results for the proposed Ti-VARe-CSV (M7) model, which is described in detail in Section 2. The model is estimated using the full sample and a Markov Chain Monte Carlo (MCMC) algorithm with 55,000 total iterations, a burn-in period of 5,000 draws, and a thinning factor of 5. Consequently, the results reported in this section are based on 10,000 posterior draws.

We begin the empirical analysis by evaluating the convergence of the proposed MCMC sampler using the well established inefficiency factor (IF) as a convergence diagnostic (Primiceri, 2005), i.e.:

$$1 + 2\sum_{l=1}^{L} \rho_l \tag{21}$$

where L is chosen sufficiently large such that the autocorrelations ρ_l taper off.

To summarize the distribution of the inefficiency factors, we present box plots. In each box plot, the central line represents the median of the distribution, while the upper and lower edges of the box correspond to the 75th and 25th percentiles, respectively. The whiskers indicate the maximum and minimum values. The results indicate that the vast majority of the inefficiency factors lie well below the commonly used threshold value of 20, suggesting that the proposed sampler generates posterior draws with relatively low autocorrelation.

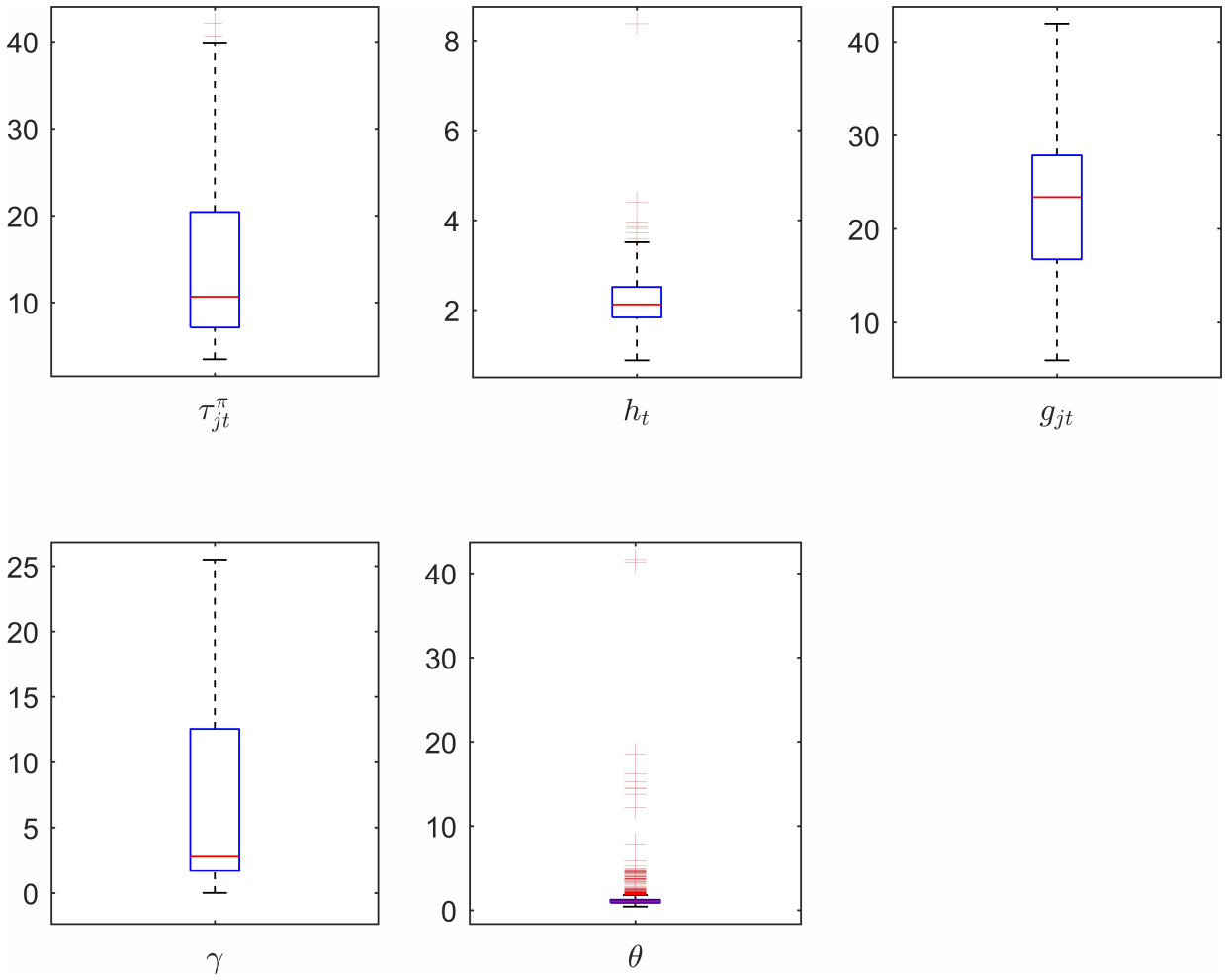

Figure 1: Box-plots of inefficiency factors of posterior draws from the Ti-VARe-CSV (M7) model. The vector $\boldsymbol{\theta}$ gathers the remaining coefficients, i.e. $\boldsymbol{\theta} = \{\text{vec}(\mathbf{B}), \text{vec}(\boldsymbol{\Sigma}), \{d_{j0}\}_{j=1}^{3}, \{d_{j1}\}_{j=1}^{3}, \}, \{\sigma_j^{\pi e}\}_{j=1}^{3}, \rho, \varphi, \{\varphi_j^{g}\}_{j=1}^{3}, \{\tau_{j0}^{\pi}\}_{j=1}^{3}, \{g_{j0}\}_{j=1}^{3}\}$

Next, Figure 2 presents the posterior means of trend inflation, $\tau_{j,t}^{\pi}$ for $j \in \text{PCE}, \text{GDPd}, \text{CPI}$, obtained from all eight model specifications reported in Table 2. The left column of Figure 2 displays the posterior means of trend inflation (red lines) together with the 68% and 95% credible intervals, the observed inflation series (blue dashed lines), and the corresponding inflation expectations proxies (black lines; see Table 1), based on the proposed M7 specification.

Overall, the estimated trend inflation series are considerably smoother than the observed inflation rates and closely track the inflation expectations proxies, particularly after 2000, across all three inflation measures. Moreover, the credible intervals for trend inflation almost always contain the corresponding inflation expectations proxy. The only exceptions occur during a few short episodes in the 1970s and early 1980s.

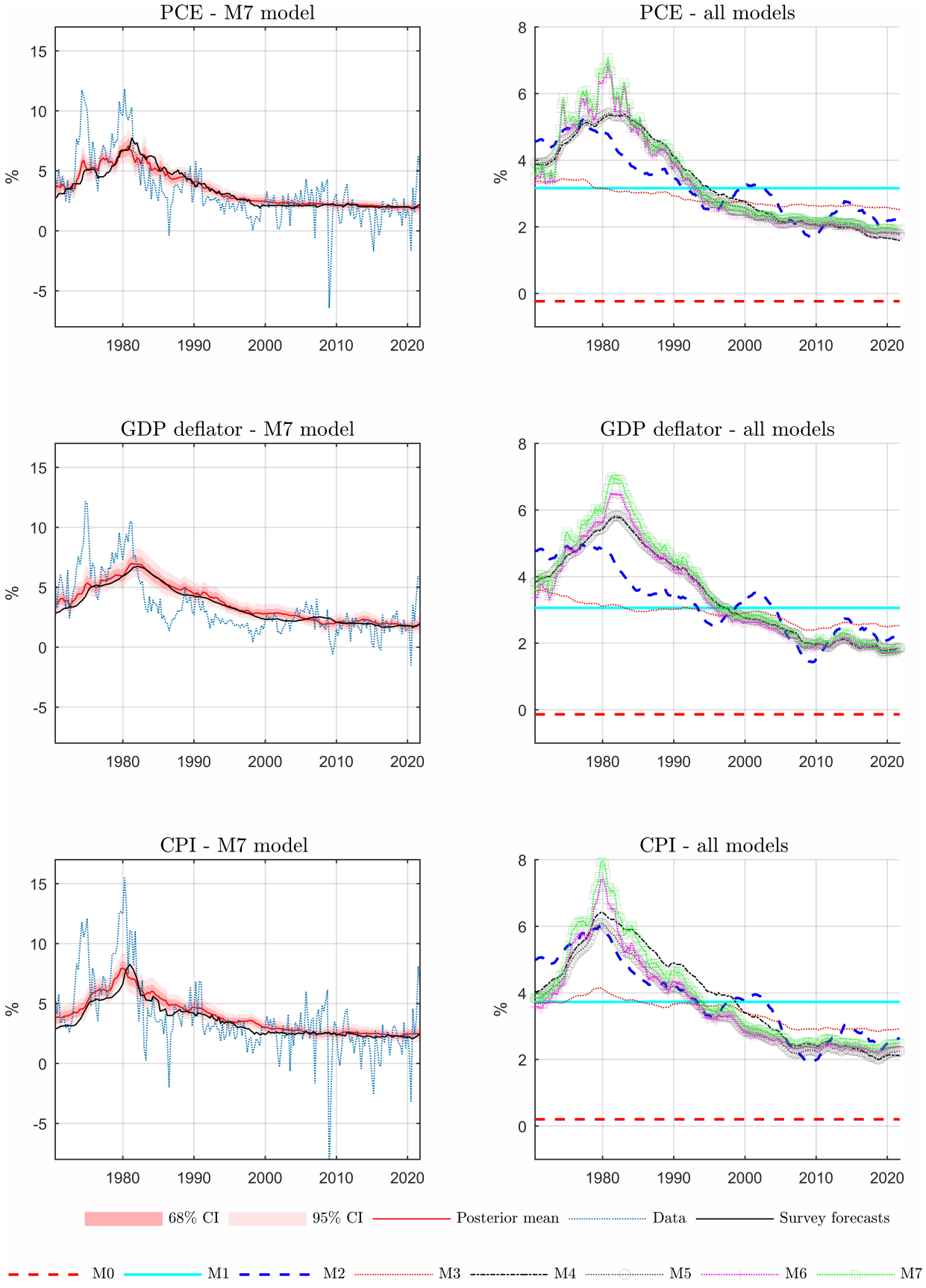

Figure 2: Posterior means of trend inflation, τ^{π}_{jt}, with $j = PCE, GDPd, CPI$ using the alternative specifications of Table 2. CI denotes the confidence interval.

Overall, our findings are broadly consistent with those of Chan et al. (2018), with one notable difference: our estimates of trend inflation do not systematically underestimate the corresponding inflation expectations proxies. This result can be understood by examining the posterior estimates of the parameters $d_{0,j}$ and $d_{1,j}$ in equation (4). Specifically, the estimated values of $d_{0,j}$ and $d_{1,j}$ are close to zero and unity, respectively, indicating that the inflation expectations proxies used in this study—namely the EWMA filter and long-run survey-based inflation forecasts—constitute approximately unbiased measures of trend inflation (see Figure E.7 in Appendix E).

Recall that Chan et al. (2018), using a univariate framework, find that long-run survey-based inflation forecasts are biased proxies for model-implied trend inflation. By contrast, our results suggest that such biases are considerably weaker in the present framework. This difference may be attributed to several factors: (i) the multivariate structure of our model and the additional information contained in the macroeconomic variables included in the system; (ii) the use of a backward-looking statistical filter (EWMA) as an alternative proxy for inflation expectations; and (iii) differences in the sample period considered.

The right column of Figure 2 presents the posterior means of trend inflation produced by the alternative model specifications reported in Table 2. A striking feature of these results is that the unconditional mean implied by the baseline M0 model is close to zero, which lies well below both the Federal Reserve's inflation target (approximately 2%) and the historical average of observed inflation.

Turning to the M1 specification, i.e., the steady-state VAR model, we observe that it tends to underestimate trend inflation during the Great Inflation period of the 1970s and early 1980s, while overestimating trend inflation during the subsequent Great Moderation and towards the end of the sample. This pattern suggests that explicitly modeling time variation in trend inflation may be beneficial even in a large cross-sectional VAR framework.

Furthermore, the trend inflation estimates produced by the M2 model exhibit the lowest degree of time variation, followed by those generated by the M3 specification. Recall that neither M2 nor M3 incorporates information from inflation expectations. By contrast, models M4 and M5—which incorporate inflation expectations through the EWMA filter and long-run survey-based forecasts, respectively—produce very similar trend inflation dynamics. In particular, both models indicate that trend inflation rises to approximately 6% (around 5% for the PCE measure) during the 1980s and stabilizes around 2% (approximately 2.5% for CPI inflation) over the last 10–15 years, broadly consistent with the Federal Reserve's inflation targeting objective.

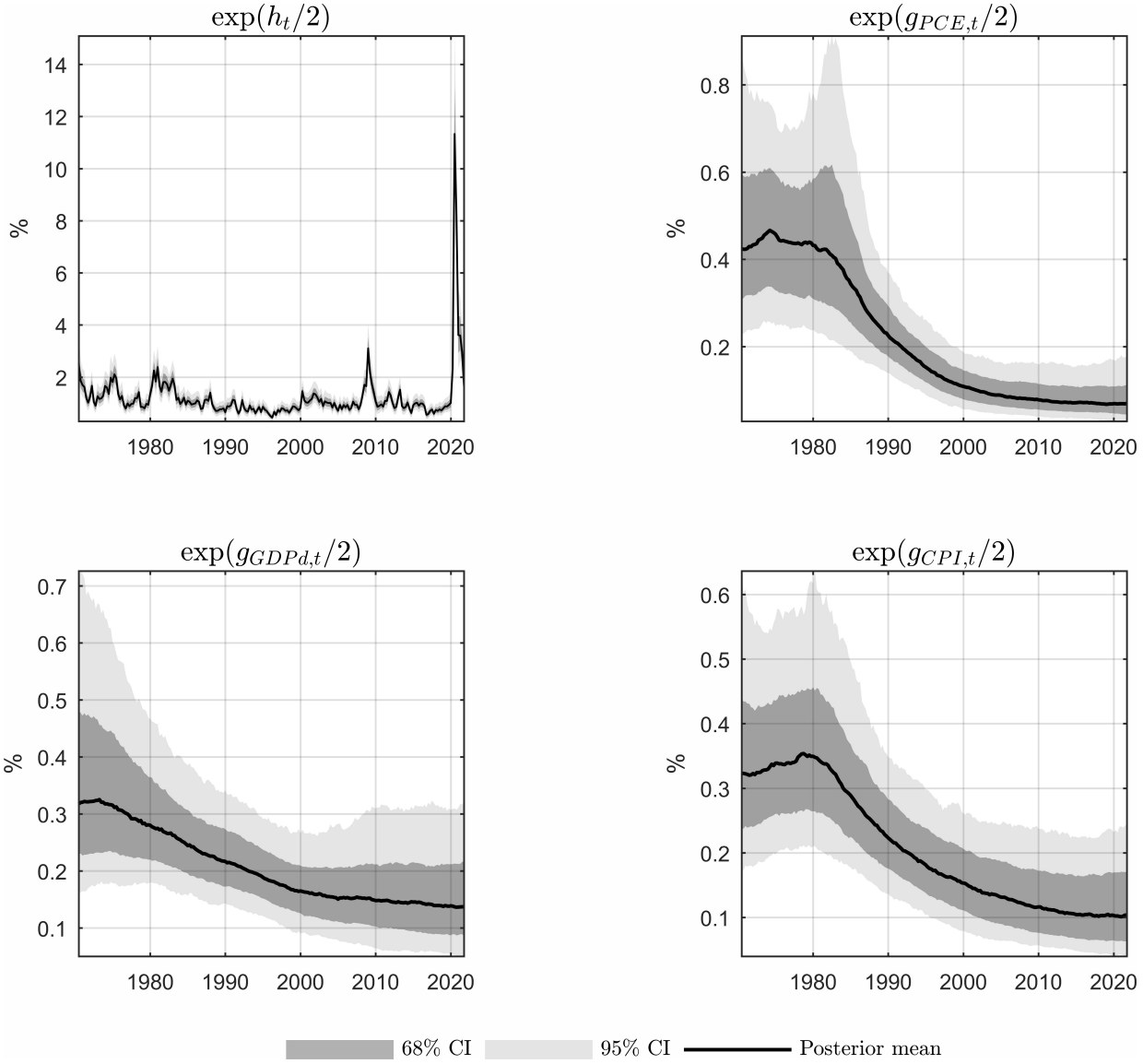

Figure 3: Posterior means of $\exp(h_t/2)$ and $\exp(g_{j,t}/2)$ with $j = PCE, GDPd, CPI$. CI denotes the confidence interval.

Finally, the posterior means of trend inflation produced by models M6 and M7 closely follow the estimates obtained from models M4 and M5 from the mid-1980s onwards and until the end of the sample period. However, during the Great Inflation period, models M6 and M7 generate higher and more volatile estimates of trend inflation. This result can be attributed to the higher levels of stochastic volatility in the error terms of equation (3). This feature is clearly illustrated in Figure 3, which reports the posterior medians of the stochastic volatility processes in the model—namely h_t and $g_{j,t}$ for $j \in$ PCE, GDPd, CPI—together with their 68% and 95% credible intervals.

4.4 Out-of-sample forecasting evaluation

In this Section we evaluate the forecasting ability of the alternative specifications of Table 2 by designing an out-of-sample forecasting exercise where we use approximately the last

40 years, i.e. from 1980 Q1 to 2021 Q3, as an evaluation period. To that end, we employ a recursive estimation of the models, generating up to 12 quarters ahead inflation forecasts, over an expanding window.

We use the mean squared error (RMSE) and the continuous ranked probability score (CRPS) to assess the point and density forecasting performance, respectively (see e.g. D. P. Louzis, 2019, for a related discussion). Figures 4, 5 and 6 present the forecasting accuracy gains in % relative to the baseline M0 model (VAR-CSV) for the PCE inflation, GDP deflator and CPI inflation metrics, respectively. We can draw a number of interesting conclusions from the forecasting results presented in Figures 4 to 6.

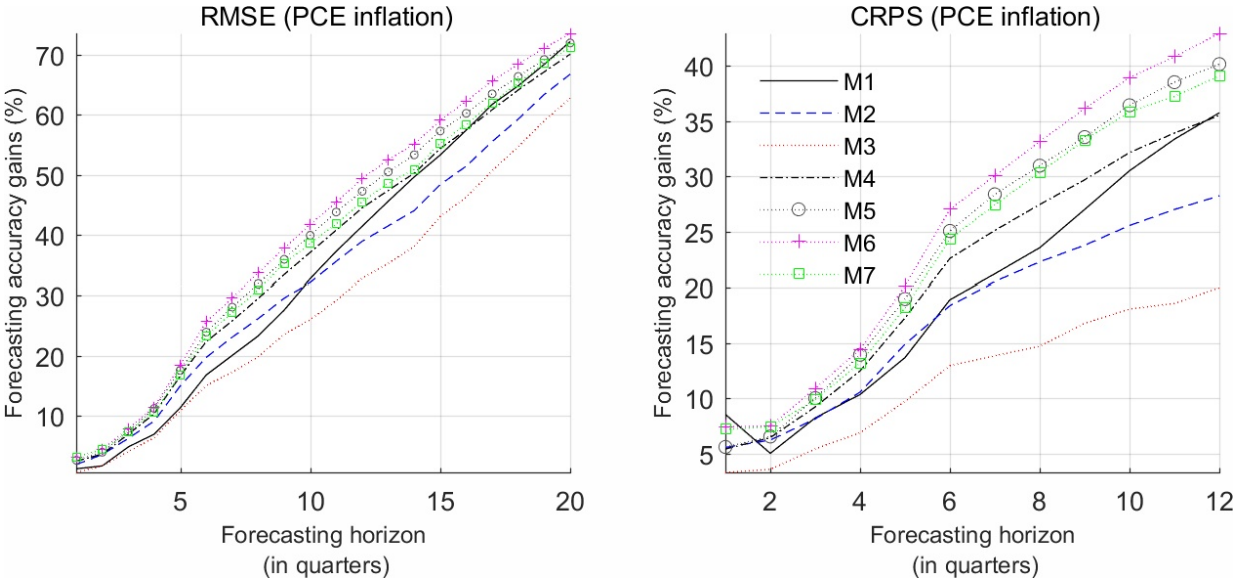

Figure 4: Out-of-sample forecasting evaluation for the PCE inflation. Figure shows the forecasting accuracy gains in % relative to the baseline M0 model (BVAR-CSV) with respect to point (RMSE) and density(CRPS) forecasting accuracy metrics. RMSE and CRPS denote the root mean squared error and continuous ranked probability score metrics, respectively. The competing models, M1 - M7, are described in Table 2.

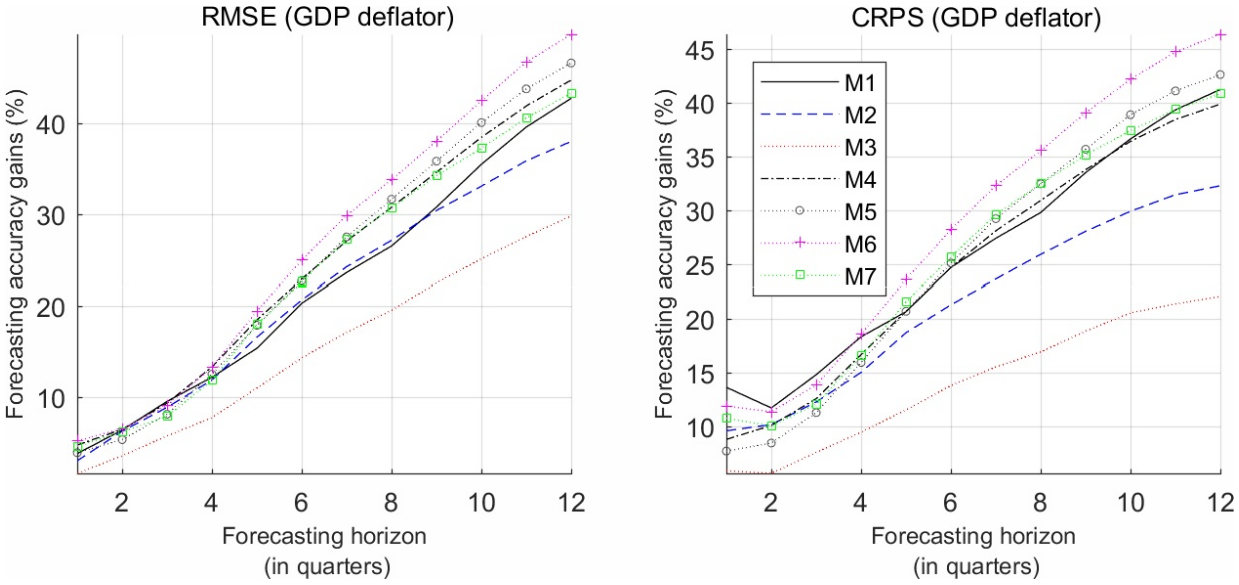

Figure 5: Out-of-sample forecasting evaluation for the GDP deflator. Figure shows the forecasting accuracy gains in % relative to the baseline M0 model (BVAR-CSV) with respect to point (RMSE) and density(CRPS) forecasting accuracy metrics. RMSE and CRPS denote the root mean squared error and continuous ranked probability score metrics, respectively. The competing models, M1 - M7, are described in Table 2.

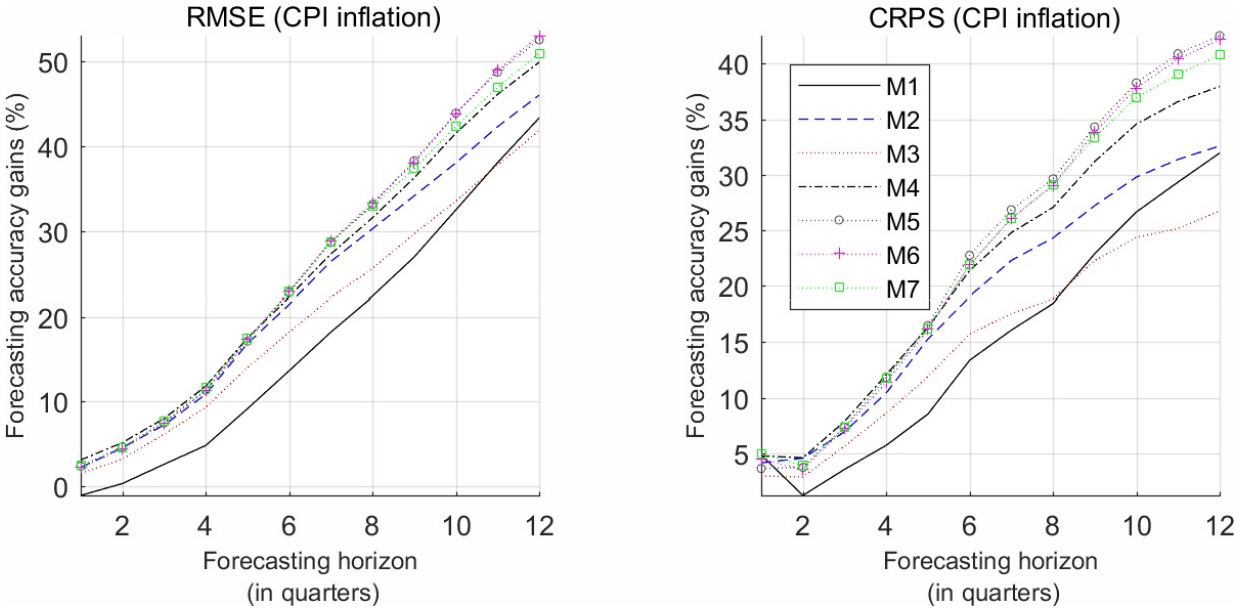

Figure 6: Out-of-sample forecasting evaluation for the CPI inflation Figure shows the forecasting accuracy gains in % relative to the baseline M0 model (BVAR-CSV) with respect to point (RMSE) and density(CRPS) forecasting accuracy metrics. RMSE and CRPS denote the root mean squared error and continuous ranked probability score metrics, respectively. The competing models, M1 - M7, are described in Table 2.

We begin with the most striking feature of all three figures: nearly all competing models outperform the baseline specification across forecasting horizons and inflation measures.

Indeed, positive forecasting accuracy gains are observed in almost all cases, with the only exception being the one-quarter-ahead RMSE for CPI inflation under the M1 specification. These results are consistent with the existing literature (see e.g. Beechey & Österholm, 2010; Villani, 2009; D. P. Louzis, 2019; Banbura & van Vlodrop, 2018, among others), which finds that steady-state priors and/or time-varying unconditional means improve macroeconomic and inflation forecasting performance. To the best of our knowledge, however, this is the first study to confirm this result within a large-VAR framework.

Another noteworthy pattern is that all models tend to generate larger forecasting gains at longer horizons relative to the baseline specification. In particular, the forecasting improvements appear to increase almost linearly with the forecast horizon across all inflation measures. This finding is also consistent with the aforementioned literature and can be attributed to the more accurate estimation of the unconditional mean provided by models M1–M7 relative to the baseline M0 model (see also Figure 2). Since the VAR model is stationary and mean-reverting, more accurate estimates of the unconditional mean translate into improved long-horizon forecasts.

We next examine whether the restrictions summarized in Table 2 materially affect forecasting performance. We begin with models M1, M2, and M3, which are consistently among the weakest performers across inflation measures and evaluation metrics. Interestingly, the M1 model (steady-state VAR) often outperforms models M2 and M3, despite the latter allowing for time-varying unconditional means. The M3 model emerges as the weakest specification overall, except in the case of CPI inflation, where the M1 model typically produces the least accurate forecasts. Nevertheless, introducing a common inflation trend in model M2 proves beneficial relative to model M3, as M2 consistently outperforms M3 across horizons.

Turning to models M4 and M5, which incorporate information from inflation expectations proxies (the EWMA filter and survey-based forecasts, respectively), the empirical results are clear: models that include inflation expectations generate substantially more accurate forecasts. In particular, forecasting accuracy gains of up to 7% are observed across forecasting horizons, inflation measures, and evaluation metrics. Moreover, model M5, which incorporates long-term survey-based inflation expectations, consistently outperforms model M4, which relies on the EWMA statistical filter.

The results also indicate that model M6, which allows for stochastic volatility in the innovations of the trend inflation equation (3), generally outperforms model M5, with the exception of CPI inflation where both models display broadly similar forecasting performance. By contrast, estimating the parameters $d_{0,j}$ and $d_{1,j}$ in the M7 specification does not lead to additional forecasting improvements. In fact, the M7 model is typically outperformed by both M6 and M5 across most forecasting horizons and inflation measures.

Overall, the forecasting results presented in this section indicate that the proposed modeling framework can deliver substantial improvements in both point and density inflation forecasts, particularly at longer forecasting horizons. The most important feature driving these improvements appears to be the incorporation of inflation expectations proxies, either through the EWMA statistical filter or through long-term survey-based forecasts, with the latter clearly providing stronger forecasting gains. Finally, imposing the restrictions $d_{0,j} = 0$ and $d_{1,j} = 1$—thereby treating inflation expectations as unbiased measures of trend inflation—further enhances the forecasting performance of the model.

5 Summary and concluding remarks

This paper develops a large trend-inflation VAR model that incorporates inflation expectations proxies in the spirit of Chan et al. (2018). The proposed framework features a hybrid trend structure in which a subset of the unconditional means is allowed to evolve over time while the remaining ones remain constant. This specification provides a flexible representation of trend dynamics while maintaining the tractability required for high-dimensional VAR systems. To estimate the model efficiently, we develop an MCMC algorithm based on recent advances in precision-based matrix methods, which allows the estimation of VAR models with a large cross-sectional dimension.

The empirical analysis relies on a dataset of twenty macroeconomic and financial variables for the U.S. economy spanning more than six decades. Using an extensive out-of-sample forecasting exercise, we show that the proposed specification consistently outperforms several benchmark large-VAR models in terms of both point and density inflation forecasts. In particular, models that incorporate proxies for inflation expectations—either through statistical filters or survey-based measures—deliver substantial forecasting gains, especially at longer horizons. The results further indicate that long-term survey-based inflation expectations contain valuable information that improves forecasting accuracy beyond what can be obtained from purely statistical trend estimates.

Overall, our findings highlight the importance of modeling trend inflation and incorporating information from inflation expectations when forecasting inflation in large macroeconomic systems. Future research could extend the proposed framework by allowing for richer expectation formation mechanisms or by applying the model to other economies and macroeconomic environments.

References

Bańbura, M., & Bobeica, E. (2022). Does the phillips curve help to forecast euro area inflation? *International Journal of Forecasting*.

Banbura, M., Brenna, F., Paredes, J., & Ravazzolo, F. (2021). Combining bayesian vars with survey density forecasts: does it pay off?

Bańbura, M., Giannone, D., & Reichlin, L. (2010). Large bayesian vector auto regressions. *Journal of Applied Econometrics*, *25*(1), 71–92.

Banbura, M., Leiva-Leon, D., & Menz, J.-O. (2021). Do inflation expectations improve model-based inflation forecasts?

Banbura, M., & van Vlodrop, A. (2018). Forecasting with bayesian vector autoregressions with time variation in the mean.

Beechey, M., & Österholm, P. (2010). Forecasting inflation in an inflation-targeting regime: A role for informative steady-state priors. *International Journal of Forecasting*, *26*(2), 248–264.

Carriero, A., Clark, T. E., & Marcellino, M. (2015). Bayesian vars: specification choices and forecast accuracy. *Journal of Applied Econometrics*, *30*(1), 46–73.

Carriero, A., Clark, T. E., & Marcellino, M. (2016a). Common drifting volatility in large bayesian vars. *Journal of Business & Economic Statistics*, *34*(3), 375–390.

Carriero, A., Clark, T. E., & Marcellino, M. (2019). Large bayesian vector autoregressions with stochastic volatility and non-conjugate priors. *Journal of Econometrics*, *212*(1), 137–154.

Chan, J. C. (2013). Moving average stochastic volatility models with application to inflation forecast. *Journal of Econometrics*, *176*(2), 162–172.

Chan, J. C. (2017). *Notes on bayesian macroeconometrics* (Tech. Rep.).

Chan, J. C. (2020a). Large bayesian vars: A flexible kronecker error covariance structure. *Journal of Business & Economic Statistics*, *38*(1), 68–79.

Chan, J. C. (2020b). *Large bayesian vector autoregressions*. Springer.

Chan, J. C. (2022). Large hybrid time-varying parameter vars. *Journal of Business & Economic Statistics*(just-accepted), 1–34.

Chan, J. C., Clark, T. E., & Koop, G. (2018). A new model of inflation, trend inflation, and long-run inflation expectations. *Journal of Money, Credit and Banking*, *50*(1), 5–53.

Chan, J. C., & Jeliazkov, I. (2009). Efficient simulation and integrated likelihood estimation in state space models. *International Journal of Mathematical Modelling and Numerical Optimisation*, *1*(1-2), 101–120.

Chan, J. C., Koop, G., & Potter, S. M. (2013). A new model of trend inflation. *Journal of Business & Economic Statistics*, *31*(1), 94–106.

Chan, J. C., Koop, G., & Potter, S. M. (2016). A bounded model of time variation in trend inflation, nairu and the phillips curve. *Journal of Applied Econometrics*, *31*(3), 551–565.

Clark, T. E., & McCracken, M. W. (2010). Averaging forecasts from vars with uncertain instabilities. *Journal of Applied Econometrics*, *25*(1), 5–29.

Clark, T. E., & McCracken, M. W. (2011). Testing for unconditional predictive ability. In M. P. Clements & D. F. Hendry (Eds.), *The oxford handbook of economic forecasting*. Oxford: Oxford Univeristy Press.

Faust, J., & Wright, J. H. (2013). Forecasting inflation. *Handbook of economic forecasting*, *2*(Part A), 3–56.

Giannone, D., Lenza, M., & Primiceri, G. E. (2015). Prior selection for vector autoregressions. *Review of Economics and Statistics*, *97*(2), 436–451.

Golub, G. H., & Van Loan, C. F. (2013). *Matrix computations* (Vol. 3). JHU press.

Hauzenberger, N., Huber, F., & Klieber, K. (2023). Real-time inflation forecasting using non-linear dimension reduction techniques. *International Journal of Forecasting*, *39*(2), 901–921.

Koop, G., & Korobilis, D. (2013). Large time-varying parameter vars. *Journal of Econometrics*, *177*(2), 185–198.

Louzis, D. (2016b). Steady-state priors and bayesian variable selection in var forecasting. *Studies in Nonlinear Dynamics & Econometrics*, *20*(5), 495–527.

Louzis, D. P. (2019). Steady-state modeling and macroeconomic forecasting quality. *Journal of Applied Econometrics*, *34*(2), 285–314.

McCracken, M., & Ng, S. (2020). *Fred-qd: A quarterly database for macroeconomic research, federal reserve bank of st* (Tech. Rep.). Louis Working Paper, 2020-005, https://doi. org/10.20955/wp.

Primiceri, G. E. (2005). Time varying structural vector autoregressions and monetary policy. *The Review of Economic Studies*, *72*(3), 821–852.

Stock, J. H., & Watson, M. W. (2007). Why has us inflation become harder to forecast? *Journal of Money, Credit and banking*, *39*, 3–33.

Villani, M. (2009). Steady-state priors for vector autoregressions. *Journal of Applied Econometrics*, *24*(4), 630–650.

Yuster, R., & Zwick, U. (2005). Fast sparse matrix multiplication. *ACM Transactions On Algorithms (TALG)*, *1*(1), 2–13.

Online Appendix

Appendix A Data description

Table A.1 presents the variables used in the empirical analysis and the respective transformation code. In particular, 1 denotes the annualized growth rates calculated as $y_t = 400\log(x_t/x_{t-1})$ and 0 denotes no transformation. The sample spans from 1959 Q2 to 2021 Q3 and all variables were retrieved from the FRED-QD database at the Federal Reserve Bank of St. Louis (McCracken & Ng, 2020).

Table A.1: Variables used in the empirical analysis

Description	Transformation code	Mnemonic
Real Gross Domestic Product	1	GDPC1
Real Personal Consumption Expenditures	1	PCECC96
Real Disposable Personal Income	1	DPIC96
Industrial Production Index	1	INDPRO
Industrial Production: Final Products	1	IPFINAL
Civilian Unemployment Rate (Percent)	0	UNRATE
All Employees: Total nonfarm	1	PAYEMS
Civilian Employment	1	CE16OV
Personal Consumption Expenditures: Chain-type Price index	1	PCECTPI
Gross Domestic Product: Chain-type Price index	1	CDPCTPI
Consumer Price Index for All Urban Consumers: All Items	1	CPIAUCSL
Producer Price Index for All commodities	1	PPIACO
Nonfarm Business Sector: Real Compensation Per Hour	1	COMPRNFB
Nonfarm Business Section: Real Output Per Hour of All Persons	1	OPHNFB
Real M2 Money Stock	1	M2REAL
10-Year Treasury Constant Maturity Rate	0	GS10
Moody's Seasoned Aaa Corporate Bond Yield (Percent)	0	AAA
Moody's Seasoned Baa Corporate Bond Yield (Percent)	0	BAA
3-Month Treasury Bill: Secondary Market Rate (Percent)	0	TB3MS
S&P's Common Stock Price Index: Composite	1	S&P 500

Appendix B Estimation details

B.1 Derivation of equations (7) and (18)

We rewrite (1) as:

$$\begin{aligned}
\boldsymbol{y}_t &= \mathbf{S}_\gamma \boldsymbol{\gamma} + \mathbf{S}_{\tau\pi}\boldsymbol{\tau}_t^\pi + \sum_{l=1}^{p} \mathbf{B}_l \left(\boldsymbol{y}_{t-l} - \mathbf{S}_\gamma \boldsymbol{\gamma} - \mathbf{S}_{\tau\pi}\boldsymbol{\tau}_{t-l}^\pi\right) + \boldsymbol{\varepsilon}_t \\
(\boldsymbol{y}_t - \mathbf{S}_\gamma \boldsymbol{\gamma}) - \sum_{l=1}^{p} \mathbf{B}_l(\boldsymbol{y}_{t-l} - \mathbf{S}_\gamma \boldsymbol{\gamma}) &= \mathbf{S}_{\tau\pi}\boldsymbol{\tau}_t^\pi - \sum_{l=1}^{p} \mathbf{B}_l \mathbf{S}_{\tau\pi}\boldsymbol{\tau}_{t-l}^\pi + \boldsymbol{\varepsilon}_t \\
\mathbf{H_B}(\boldsymbol{y} - (\mathbf{1}_T \otimes \mathbf{S}_\gamma)\gamma) &= \mathbf{H_B}(\mathbf{I}_T \otimes \mathbf{S}_{\tau\pi})\boldsymbol{\tau}^\pi + \boldsymbol{\varepsilon}
\end{aligned} \tag{B.1}$$

which gives (7).

Alternatively, we can also write (1) as:

$$\begin{aligned}
(\boldsymbol{y}_t - \mathbf{S}_{\tau\pi}\boldsymbol{\tau}_t^\pi) - \sum_{l=1}^{p} \mathbf{B}_l(\boldsymbol{y}_{t-l} - \mathbf{S}_{\tau\pi}\boldsymbol{\tau}_{t-l}^\pi) &= \mathbf{S}_\gamma \boldsymbol{\gamma} - \sum_{l=1}^{p} \mathbf{B}_l \mathbf{S}_\gamma \boldsymbol{\gamma} + \boldsymbol{\varepsilon}_t \\
\mathbf{H_B}(\boldsymbol{y} - \mathbf{I}_T \otimes \mathbf{S}_{\tau\pi}) &= \mathbf{H_B}(\mathbf{1}_T \otimes \mathbf{S}_\gamma)\gamma + \boldsymbol{\varepsilon}
\end{aligned} \tag{B.2}$$

which gives (18).

Appendix C Propositions

To prove Propositions C.1 andC.2 we rely on Lemma C.1 by Yuster and Zwick (2005, p. 5) on sparse matrix multiplication.

Lemma C.1. *The multiplication of any* $\mathbf{K} \in \mathbb{R}^{m\times l}$, $\mathbf{\Lambda} \in \mathbb{R}^{l\times n}$ *sparse matrices requires* $\sum_{r=1}^{l} \boldsymbol{\kappa}_r \boldsymbol{\lambda}_r$ *multiplications, where* $\boldsymbol{\kappa}_r$ *is the number of non-zero elements in the* r*-th column of* $\mathbf{K}$ *and* $\boldsymbol{\lambda}_r$ *are the number of non-zero elements in the* r*-th row of* $\mathbf{\Lambda}$*.*

Proposition C.1. *Let* $\mathbf{B}_i \in \mathbb{R}^{n\times n}$, $\mathbf{S}_{\tau\pi} \in \{0,1\}^{n\times q}$ *be a binary selection matrix,* $\bar{\mathbf{S}}_{\tau\pi} = \mathbf{I}_T \otimes \mathbf{S}_{\tau\pi} \in \{0,1\}^{nT\times qT}$, $\mathbf{H_B} \in \mathbb{R}^{nT\times nT}$ *be a band matrix defined in* (8) *and* $n, T, q, p \in \mathbb{Z}^+$*. Then calculating the sparse matrix product* $\mathbf{H_B}\bar{\mathbf{S}}_{\tau\pi}$ *requires* $\mathcal{O}(p(T-(p+1)/2)nq)$ *arithmetic operations. Alternatively, we can calculate* $\mathbf{H_B}\bar{\mathbf{S}}_{\tau\pi}$ *relying only on the multiplications of* $\mathbf{B}_i$ *and* $\mathbf{S}_{\tau\pi}$*, i.e.* $\mathbf{B}_i\mathbf{S}_{\tau\pi}$*,* $i = 1, ..., p$*, which requires* $\mathcal{O}(pnq)$ *operations;* $\mathcal{O}(q\{np[T-1-(p-1)/2]+T\}) > \mathcal{O}(pnq)$ *if* $T > (p+3)/2$*.*

Proof. To calculate the order-of-magnitude, $\mathcal{O}(.)$, we focus on the number of multiplications required to calculate $\mathbf{H_B}\bar{\mathbf{S}}_{\tau\pi}$ since these involve the highest order operations. Multiplications typically tend to dominate the overall computation procedure because the number of additions required is always bounded by the number of the required multiplications (see Golub and Van Loan (2013, p. 12) and Yuster and Zwick (2005, p. 5) for details)

Thus, according to Lemma C.1, in order to calculate the number of multiplications for $\mathbf{H_B}\bar{\mathbf{S}}_{\tau\pi}$, it suffices to compute the number of non-zero entries for each of the columns and

rows of $\mathbf{H}_B$ and $\bar{\mathbf{S}}_{\tau\pi}$, respectively. To that end, it would be helpful to write the product $\mathbf{H_B}\bar{\mathbf{S}}_{\tau\pi}$ analytically:

$$\mathbf{H_B}\bar{\mathbf{S}}_{\tau\pi} = \underbrace{\begin{bmatrix} \mathbf{I}_n & \dots & \mathbf{0} & \mathbf{0} & \dots & \mathbf{0} \\ -\mathbf{B}_1 & \mathbf{I}_n & \mathbf{0} & \mathbf{0} & \dots & \mathbf{0} \\ -\mathbf{B}_2 & -\mathbf{B}_1 & \mathbf{I}_n & \mathbf{0} & \dots & \mathbf{0} \\ \vdots & \vdots & \dots & \ddots & \dots & \vdots \\ \vdots & -\mathbf{B}_p & \dots & -\mathbf{B}_1 & \mathbf{I}_n & \mathbf{0} \\ \mathbf{0} & \dots & -\mathbf{B}_p & \dots & -\mathbf{B}_1 & \mathbf{I}_n \end{bmatrix}}_{nT\times nT} \underbrace{\begin{bmatrix} \mathbf{S}_{\tau\pi} & \mathbf{0} & \mathbf{0} & \dots & \mathbf{0} & \mathbf{0} \\ \mathbf{0} & \mathbf{S}_{\tau\pi} & \mathbf{0} & \dots & \mathbf{0} & \mathbf{0} \\ \mathbf{0} & \mathbf{0} & \mathbf{S}_{\tau\pi} & \dots & \mathbf{0} & \mathbf{0} \\ \vdots & \ddots & \ddots & \ddots & \mathbf{0} & \mathbf{0} \\ \mathbf{0} & \mathbf{0} & \dots & \mathbf{0} & \mathbf{S}_{\tau\pi} & \mathbf{0} \\ \mathbf{0} & \mathbf{0} & \dots & \mathbf{0} & \mathbf{0} & \mathbf{S}_{\tau\pi} \end{bmatrix}}_{nT\times qT} \tag{C.1}$$

Obviously, for each of the first $n(T-p)$ columns of $\mathbf{H}_B$ we can find $np+1$ non-zeros entries, where p is the number of lags, n is the number of variables and unity comes from the identity matrix in the main diagonal of $\mathbf{H_B}$. For instance, for the first column of $\mathbf{H_B}$, i.e. $\mathbf{c}_{HB,1}$, we have:

$$\mathbf{c}_{HB,1} = [\underbrace{1, ..., 0}_{1 \text{ element } \neq 0}, \underbrace{B_{11,1}, B_{21,1}, ..., B_{n1,1}, B_{11,2}, B_{21,2}, ..., B_{n1,2}, ..., B_{11,p}, B_{21,p}, ..., B_{n1,p}}_{n\times p \text{ elements } \neq 0}, \underbrace{0, ..., 0, ...0, ..., 0}_{n\times(T-p-1) \text{ zeros}}]'$$

where $\{B_{ij,l}\}_{i,j=1}^{n}$ is $ij-th$ element of coefficient matrix $\boldsymbol{B}_l$.

Now, by definition the selection matrix $\bar{\mathbf{S}}_{\tau\pi}$ has either one non-zero element in each row or none. It also holds that for each n rows there are only q rows with one non-zero element. This practically means that for the first n rows (columns) and assuming that all non-zeros entries are gathered at the end, the number of required multiplications is (see Lemma C.1):

$$\begin{aligned} c_{HB,1}\cdot r_{S,1} + ... + c_{HB,n}\cdot r_{S,n} &= \underbrace{c_{HB,1}\cdot 0 + ... + c_{HB,n-q}\cdot 0}_{(n-q) \text{ times}} + ... \\ &+ \underbrace{c_{HB,n-q+1}\cdot 1 +, ..., + c_{HB,n}\cdot 1}_{q \text{ times}} \\ &= \sum_{k=1}^{q} c_{HB,k} = \sum_{k=1}^{q} np + 1 = q(np+1) \end{aligned}$$

where $c_{HB,k}$ and $r_{S,k}$ are the $k-th$ column and row of $\mathbf{H_B}$ and $\bar{\mathbf{S}}_{\tau\pi}$ respectively. It is trivial to generalize this results for the first $n(T-p)$ rows (columns):

$$\sum_{k=1}^{n(T-p)} c_{HB,k}\cdot r_{S,k} = \sum_{k=1}^{q(T-p)} c_{HB,k} = \sum_{k=1}^{q(T-p)} (np+1) = q(T-p)(np+1) \tag{C.2}$$

where $c_{HB,k}$ and $r_{S,k}$ are the $k-th$ column and row of $\mathbf{H_B}$ and $\bar{\mathbf{S}}_{\tau\pi}$ respectively.

Next, we calculate the non-zero entries for the last np columns of $\mathbf{H_B}$. In particular, we pin down a specific pattern which is repeated $p-1$ times every n columns. That is, from column $k = n(T-p)+1$ to column $k = n(T-p+1)$ we have $c_{HB,r} = n(p-1)+1$ non-zero entries meaning that the required number of multiplications is:

$$\sum_{k=n(T-p)+1}^{n(T-p+1)} c_{HB,k}\cdot r_{S,k} = \sum_{k=1}^{q} n(p-1)+1 = q[n(p-1)+1] \tag{C.3}$$

For the next n columns, i.e. from $k = n(T-p+1)+1$ to $k = n(T-p+2)$, the number of non-zero elements in each column is $c_{HB,k} = n(p-2)+1$; likewise from $k = n(T-p+(j-1))+1$ to $k = n(T-p+j)$ for $j = 1, ..., p-1$ we have $c_{HB,k} = n(p-j)+1$ non zero elements, thus, implying that the required number of multiplications is:

$$\begin{aligned}
\sum_{k=n(T-p+1)+1}^{n(T-p+2)} c_{HB,k} \cdot r_{S,k} &= \sum_{k=1}^{q} n(p-2)+1 = q[n(p-2)+1] \\
&\dots \\
\sum_{k=n(T-p+(j-1))+1}^{n(T-p+j)} c_{HB,k} \cdot r_{S,k} &= \sum_{k=1}^{q} q(p-j)+1 = q\left[n(p-j)+1\right]
\end{aligned} \tag{C.4}$$

Therefore, from (C.3) and (C.4) and also adding q multiplications required for the last n columns, we can compute the total number of multiplications for the last np columns (rows) of $\mathbf{H}_B \bar{\boldsymbol{y}}_\gamma$ as :

$$\begin{aligned}
q + \sum_{k=n(T-p)+1}^{n(T-1)} c_{HB,k} \cdot r_{S,k} &= q + \sum_{j=1}^{p-1} q[n(p-j)+1] \\
&= q + (p-1)q(np+1) - qn\sum_{j=1}^{p-1} j = \\
&= q[1 + (p-1)(np+1) - np(p-1)/2]
\end{aligned} \tag{C.5}$$

Now, summing up (C.2) and (C.5) we get the total number of multiplications required in order to calculate $\mathbf{H_B}\bar{\mathbf{S}}_{\tau\pi}$, i.e.:

$$\begin{aligned}
\sum_{k=1}^{nT} c_{HB,k} \cdot r_{S,k} &= q(T-p)(np+1) + q[1 + (p-1)(np+1) - np(p-1)/2] \\
&= q[(T-p)(np+1) + 1 + (p-1)(np+1) - np(p-1)/2] \\
&= q\{np[T - 1 - (p-1)/2] + T\}
\end{aligned} \tag{C.6}$$

Alternatively, we can write the product $\mathbf{H_B}\bar{\mathbf{S}}_{\tau\pi}$ analytically as:

$$\mathbf{H_B}\bar{\mathbf{S}}_{\tau\pi} = \underbrace{\begin{bmatrix}
\mathbf{S}_{\tau\pi} & \mathbf{0} & \mathbf{0} & \dots & \mathbf{0} \\
-\mathbf{B}_1\mathbf{S}_{\tau\pi} & \mathbf{S}_{\tau\pi} & \mathbf{0} & \dots & \mathbf{0} \\
-\mathbf{B}_2\mathbf{S}_{\tau\pi} & -\mathbf{B}_1\mathbf{S}_{\tau\pi} & \mathbf{S}_{\tau\pi} & \dots & \mathbf{0} \\
\vdots & \ddots & \ddots & \ddots & \mathbf{0} \\
\mathbf{0} & -\mathbf{B}_p\mathbf{S}_{\tau\pi} & \dots & -\mathbf{B}_1\mathbf{S}_{\tau\pi} & \mathbf{S}_{\tau\pi}
\end{bmatrix}}_{nT \times qT} \tag{C.7}$$

Therefore, we can first compute $\mathbf{B}_i\mathbf{S}_{\tau\pi}$, for $i = 1, ...p$, which requires only qnp multiplications, and then construct the matrix in (C.7).[11]

[11] The construction of both $\mathbf{H_B}$ and the matrix in (C.7) requires a *for loop* of p iterations in Matlab with identical computation time for both cases. Thus, the computational efficiency of the two alternative ways of computing $\mathbf{H_B}\bar{\mathbf{S}}_{\tau\pi}$ does not depend upon the construction process of either matrices.

Therefore, we have shown that calculating $\mathbf{H_B}\bar{\mathbf{S}}_{\tau\pi}$ involves $\mathcal{O}(q\{np[T-1-(p-1)/2]+T\})$ or $\mathcal{O}(qnp)$ arithmetic operations, depending on the method we choose, because, as we also mentioned above, the number of additions required is always bounded by the number of the required multiplications (see Golub and Van Loan (2013, p. 12) and Yuster and Zwick (2005, p. 5) for details).

Now, to prove Proposition C.1 suffices to prove that $q\{np[T-1-(p-1)/2]+T > qnp$, i.e. we have to show that:

$$\begin{aligned} &np[T-1-(p-1)/2]+T > np \Leftrightarrow \\ &np[T-2-(p-1)/2]+T > 0 \end{aligned} \tag{C.8}$$

Because $n, T, q, p \in \mathbb{Z}^+$ by definition the inequality in (C.8) also holds if we show that the quantity in the bracket is also a positive number, i.e.:

$$\begin{aligned} T-2-(p-1)/2 > 0 \Leftrightarrow \\ T > (p+3)/2 \end{aligned} \tag{C.9}$$

(C.9) proves Proposition C.1. □

Proposition C.2. *Let $\mathbf{S}_\gamma \in \{0,1\}^{n\times(n-q)}$ be a binary selection matrix, $\bar{\mathbf{S}}_\gamma = \mathbf{1}_T \otimes \mathbf{S}_\gamma \in \{0,1\}^{nT\times(n-q)}$, $\mathbf{B}_i$ and $\mathbf{H_B}$ are defined in Proposition C.1 with $n, T, q, p \in \mathbb{Z}^+$. Then calculating the sparse matrix product $\mathbf{H_B}\bar{\mathbf{S}}_\gamma$ requires $\mathcal{O}(q\{np[T-1-(p-1)/2]+T\})$ arithmetic operations. Alternatively, we can calculate $\mathbf{H_B}\bar{\mathbf{S}}_\gamma$ based only on the multiplications of $\mathbf{B}_i$ and $\mathbf{S}_\gamma$, i.e. $\mathbf{B}_i\mathbf{S}_\gamma$, for $i = 1, ..., p$, which requires $\mathcal{O}(pnm)$ operations; $\mathcal{O}(q\{np[T-1-(p-1)/2]+T\}) > \mathcal{O}(pnm)$ if $T > (p+3)/2$.*

Proof. As in Proposition C.1 we write analytically:

$$\begin{aligned} \mathbf{H_B}\bar{\mathbf{S}}_\gamma &= \underbrace{\begin{bmatrix} \mathbf{I}_n & \mathbf{0} & \dots & \dots & \mathbf{0} \\ -\mathbf{B}_1 & \mathbf{I}_n & \mathbf{0} & \dots & \mathbf{0} \\ -\mathbf{B}_2 & -\mathbf{B}_1 & \mathbf{I}_n & \dots & \mathbf{0} \\ \vdots & \vdots & \ddots & \ddots & \mathbf{0} \\ \mathbf{0} & -\mathbf{B}_p & \dots & -\mathbf{B}_1 & \mathbf{I}_n \end{bmatrix}}_{nT\times nT} \underbrace{\begin{bmatrix} \mathbf{S}_\gamma \\ \mathbf{S}_\gamma \\ \mathbf{S}_\gamma \\ \vdots \\ \mathbf{S}_\gamma \end{bmatrix}}_{nT\times(n-q)} \\ &= \underbrace{\begin{bmatrix} \mathbf{S}_\gamma \\ -\mathbf{B}_1\mathbf{S}_\gamma + \mathbf{S}_\gamma \\ -\mathbf{B}_2\mathbf{S}_\gamma - \mathbf{B}_1\mathbf{S}_\gamma + \mathbf{S}_\gamma \\ -\mathbf{B}_p\mathbf{S}_\gamma \cdots - \mathbf{B}_1\mathbf{S}_\gamma + \mathbf{S}_\gamma \\ \vdots \\ -\mathbf{B}_p\mathbf{S}_\gamma - \mathbf{B}_1\mathbf{S}_\gamma + \mathbf{S}_\gamma \end{bmatrix}}_{nT\times(n-q)} \end{aligned} \tag{C.10}$$

Working similarly with Proposition C.1 it is trivial to show that the sparse matrix multiplication $\mathbf{H_B}\bar{\mathbf{S}}_\gamma$ is also $\mathcal{O}(q\{np[T-1-(p-1)/2]+T\})$, while relying only on the multiplications of $\mathbf{B}_i$ and $\mathbf{S}_\gamma$ is again $\mathcal{O}(pnm)$. This means that the proof is identical to that of Proposition C.1. □

Proposition C.3. *Let $\mathbf{B}_i$ and $\mathbf{H_B}$ be defined as in Proposition C.1, $\boldsymbol{x} = (\boldsymbol{x}_1', ..., \boldsymbol{x}_T')'$ with $\boldsymbol{x} \in \mathbb{R}^{nT\times 1}$, $\boldsymbol{x}_i \in \mathbb{R}^{n\times 1}$ and $n, T, p \in \mathbb{Z}^+$. Then calculating the sparse matrix-vector product*

$\mathbf{H_B}\boldsymbol{x}$ *requires* $\mathcal{O}(n\{np[T-1-(p-1)/2]+T\})$ *arithmetic operations. Alternatively, we can calculate* $\mathbf{H_B}\boldsymbol{x}$ *as* $(\bar{\boldsymbol{x}}_1', ..., \bar{\boldsymbol{x}}_T')'$ *where* $\bar{\boldsymbol{x}}_t = \boldsymbol{x}_t - \sum_{i=1}^{p} \boldsymbol{B}_i \boldsymbol{y}_{t-i}$ *and* $\boldsymbol{x}_0 = \boldsymbol{x}_{-1} =, ..., \boldsymbol{x}_{1-p} = \mathbf{0}$*, which requires* $\mathcal{O}(n^2p[T-(p+1)/2])$ *operations; it always holds that* $\mathcal{O}(n\{np[T-1-(p-1)/2]+T\}) > \mathcal{O}(n^2p[T-(p+1)/2])$*.*

Proof. Working similarly with Proposition C.1 and underlining that $\boldsymbol{x}$ is a dense column vector with the number of non-zero entries in its k-th row being always unity, we can calculate the number of multiplications in the $\mathbf{H_B}\boldsymbol{x}$ product as:

$$\begin{aligned}\sum_{k=1}^{nT} c_{HB,k} \cdot r_{x,k} &= \sum_{k=1}^{n(T-p)} c_{HB,k} + \sum_{k=n(T-p)+1}^{nT} c_{HB,k} \\ &= n(T-p)(np+1) + n[1+(p-1)(np+1) - np(p-1)/2] \\ &= n\{np[T-1-(p-1)/2]+T\}\end{aligned} \tag{C.11}$$

C.11 proves that $\mathbf{H_B}\boldsymbol{x}$ requires $\mathcal{O}(n\{np[T-1-(p-1)/2]+T\})$ arithmetic operations.

Alternatively we can write $\mathbf{H_B}\boldsymbol{x}$ analytically as:

$$\begin{aligned}\mathbf{H_B}\boldsymbol{x} &= \underbrace{\begin{bmatrix} \mathbf{I}_n & \mathbf{0} & \dots & \dots & \mathbf{0} \\ -\mathbf{B}_1 & \mathbf{I}_n & \mathbf{0} & \dots & \mathbf{0} \\ -\mathbf{B}_2 & -\mathbf{B}_1 & \mathbf{I}_n & \dots & \mathbf{0} \\ \vdots & \vdots & \ddots & \ddots & \mathbf{0} \\ \mathbf{0} & -\mathbf{B}_p & \dots & -\mathbf{B}_1 & \mathbf{I}_n \end{bmatrix}}_{nT \times nT} \underbrace{\begin{bmatrix} \boldsymbol{x}_1 \\ \boldsymbol{x}_2 \\ \boldsymbol{x}_3 \\ \vdots \\ \boldsymbol{x}_T \end{bmatrix}}_{nT \times 1} \\ &= \underbrace{\begin{bmatrix} \boldsymbol{x}_1 \\ -\mathbf{B}_1\boldsymbol{x}_1 + \boldsymbol{x}_2 \\ -\mathbf{B}_2\boldsymbol{x}_1 - \mathbf{B}_1\boldsymbol{x}_2 + \boldsymbol{x}_3 \\ -\mathbf{B}_p\boldsymbol{x}_1 \cdots - \mathbf{B}_1\boldsymbol{x}_p + \boldsymbol{x}_{p+1} \\ \vdots \\ -\mathbf{B}_p\boldsymbol{x}_{T-p} - \mathbf{B}_1\boldsymbol{x}_{T-1} + \boldsymbol{x}_T \end{bmatrix}}_{nT \times 1}\end{aligned} \tag{C.12}$$

Each of the rows in C.12 can be written as $\bar{\boldsymbol{x}}_t = \boldsymbol{x}_t - \sum_{i=1}^{p} \boldsymbol{B}_i \boldsymbol{y}_{t-i}$ with $\boldsymbol{x}_0 = \boldsymbol{x}_{-1} = , ..., \boldsymbol{x}_{1-p} = \mathbf{0}$ proving that $\mathbf{H_B}\boldsymbol{x}$ can be alternatively computed as $(\bar{\boldsymbol{x}}_1', ..., \bar{\boldsymbol{x}}_T')'$.

Obviously for the last $n(T-p)$ rows in (C.12) we need $(T-p)n^2p$ multiplications, since the n-sized matrix-vector multiplication is $\mathcal{O}(n^2)$, while for the first p rows we need $p(p-1)n^2/2$ multiplications. Therefore, the total number of required multiplications is:

$$(T-p)n^2p + n^2p(p-1)/2 = n^2p[T-(p+1)/2] \tag{C.13}$$

Finally, to prove that $\mathcal{O}(n\{np[T-1-(p-1)/2]+T\}) > \mathcal{O}(n^2p[T-(p+1)/2])$, it suffices to prove:[12]

$$\begin{aligned} n\{np[T-1-(p-1)/2]+T\} > (T-p)n^2p + n^2p(p-1)/2 \Leftrightarrow \\ n^2p(T-1) - n^2p(p-1)/2 + nT - n^2p(T-p) - n^2p(p-1)/2 > 0 \Leftrightarrow \\ n^2p(p-1) - 2[n^2p(p-1)/2] + nT > 0 \Leftrightarrow \\ nT > 0 \end{aligned} \tag{C.14}$$

which is true by definition because $n, T, p \in \mathbb{Z}^+$. □

[12] To prove the inequality it is more convenient to work with $(T-p)n^2p + n^2p(p-1)/2$ instead of $n^2p[T-(p+1)/2]$

Appendix D Description of the alternative specifications

This appendix provides more details on the alternative (restricted) models synopsized in Table 2 of the main text.

- **M0 model**: We start from the baseline VAR-CSV model of Chan (2020a) which is defined as:

$$\boldsymbol{y}_t = \boldsymbol{c} + \sum_{l=1}^{p} \mathbf{B}_l \boldsymbol{y}_{t-l} + \boldsymbol{\varepsilon}_t \qquad \boldsymbol{\varepsilon}_t \sim \mathcal{N}(\mathbf{0}, \exp(h_t)\boldsymbol{\Sigma}) \tag{D.1}$$

$$h_t = \rho h_{t-1} + \eta_t, \quad |\rho| < 1 \qquad \eta_t \sim \mathcal{N}(0, \varphi) \tag{D.2}$$

  where $\boldsymbol{c}$ is a $n \times 1$ vector of constant terms and the unconditional mean of the process is given by $\boldsymbol{\gamma} = (\mathbf{I}_n - \mathbf{B}_1 - ... - \mathbf{B}_p)^{-1}\boldsymbol{c}$; the uncodntinal mean, $\boldsymbol{\gamma}$, is almost solely driven by data since we typically use a flat prior on $\boldsymbol{c}$.

- **M1 model**: By imposing $\mathbf{S}_\gamma = \mathbf{I}_n$ and $\mathbf{S}_{\tau\pi} = \mathbf{0}$ we get the steady-state VAR-CSV model (Villani, 2009; D. P. Louzis, 2019):

$$\boldsymbol{y}_t = \boldsymbol{\gamma} + \sum_{l=1}^{p} \mathbf{B}_l (\boldsymbol{y}_{t-l} - \boldsymbol{\gamma}) + \boldsymbol{\varepsilon}_t \qquad \boldsymbol{\varepsilon}_t \sim \mathcal{N}(\mathbf{0}, \exp(h_t)\boldsymbol{\Sigma}) \tag{D.3}$$

$$h_t = \rho h_{t-1} + \eta_t, \quad |\rho| < 1 \qquad \eta_t \sim \mathcal{N}(0, \varphi) \tag{D.4}$$

- **M2 model**: In M2 model we consider a common trend inflation VAR (cTi-VAR) defined as:

$$\boldsymbol{y}_t = \boldsymbol{\tau}_t + \sum_{l=1}^{p} \mathbf{B}_l \left(\boldsymbol{y}_{t-l} - \boldsymbol{\tau}_{t-l}\right) + \boldsymbol{\varepsilon}_t, \qquad \boldsymbol{\varepsilon}_t \sim \mathcal{N}(\mathbf{0}, \exp(h_t)\boldsymbol{\Sigma}) \tag{D.5}$$

$$\boldsymbol{\tau}_t = \mathbf{S}_\gamma \boldsymbol{\gamma} + \mathbf{S}_{\tau\pi} \boldsymbol{\tau}_t^{\pi} \tag{D.6}$$

$$\tau_{jt}^{\pi id} = \tau_{jt-1}^{\pi id} + \epsilon_{jt}^{\tau\pi id}, \quad j = 1, ..., q, \qquad \epsilon_{jt}^{\tau\pi id} \sim \mathcal{N}(0, q_{jt}^{id}) \tag{D.7}$$

$$\tau_t^{\pi c} = \tau_{t-1}^{\pi c} + \epsilon_t^{\tau\pi c}, \qquad \epsilon_t^{\tau\pi c} \sim \mathcal{N}(0, q_t^c) \tag{D.8}$$

$$\tau_{jt}^{\pi} = \tau_t^{\pi c} + \tau_{jt}^{\pi i} \tag{D.9}$$

  where $\tau_t^{\pi c}$ is a common trend inflation factor and $\tau_{jt}^{\pi id}$ is the idiosyncratic trend inflation for each $j = GDP, CPI, PCE$ inflation measure. Now, given the ranking of the variables in Table 2, the selection matrices $\mathbf{S}_{\tau\pi}$ and $\mathbf{S}_\gamma$ are the following (20×4) and (20×17) matrices respectively:

$$\mathbf{S}_{\tau\pi} = \begin{bmatrix} 0 & 0 & 0 & 0 \\ 0 & 0 & 0 & 0 \\ 0 & 0 & 0 & 0 \\ 0 & 0 & 0 & 0 \\ 0 & 0 & 0 & 0 \\ 0 & 0 & 0 & 0 \\ 0 & 0 & 0 & 0 \\ 0 & 0 & 0 & 0 \\ 1 & 0 & 0 & 1 \\ 0 & 1 & 0 & 1 \\ 0 & 0 & 1 & 1 \\ 0 & 0 & 0 & 0 \\ 0 & 0 & 0 & 0 \\ 0 & 0 & 0 & 0 \\ 0 & 0 & 0 & 0 \\ 0 & 0 & 0 & 0 \\ 0 & 0 & 0 & 0 \\ 0 & 0 & 0 & 0 \\ 0 & 0 & 0 & 0 \end{bmatrix} \text{ and } \mathbf{S}_{\gamma} = \begin{bmatrix} 1 & 0 & 0 & 0 & 0 & 0 & 0 & 0 & 0 & 0 & 0 & 0 & 0 & 0 & 0 & 0 & 0 & 0 \\ 0 & 1 & 0 & 0 & 0 & 0 & 0 & 0 & 0 & 0 & 0 & 0 & 0 & 0 & 0 & 0 & 0 & 0 \\ 0 & 0 & 1 & 0 & 0 & 0 & 0 & 0 & 0 & 0 & 0 & 0 & 0 & 0 & 0 & 0 & 0 & 0 \\ 0 & 0 & 0 & 1 & 0 & 0 & 0 & 0 & 0 & 0 & 0 & 0 & 0 & 0 & 0 & 0 & 0 & 0 \\ 0 & 0 & 0 & 0 & 1 & 0 & 0 & 0 & 0 & 0 & 0 & 0 & 0 & 0 & 0 & 0 & 0 & 0 \\ 0 & 0 & 0 & 0 & 0 & 1 & 0 & 0 & 0 & 0 & 0 & 0 & 0 & 0 & 0 & 0 & 0 & 0 \\ 0 & 0 & 0 & 0 & 0 & 0 & 1 & 0 & 0 & 0 & 0 & 0 & 0 & 0 & 0 & 0 & 0 & 0 \\ 0 & 0 & 0 & 0 & 0 & 0 & 0 & 1 & 0 & 0 & 0 & 0 & 0 & 0 & 0 & 0 & 0 & 0 \\ 0 & 0 & 0 & 0 & 0 & 0 & 0 & 0 & 0 & 0 & 0 & 0 & 0 & 0 & 0 & 0 & 0 & 0 \\ 0 & 0 & 0 & 0 & 0 & 0 & 0 & 0 & 0 & 0 & 0 & 0 & 0 & 0 & 0 & 0 & 0 & 0 \\ 0 & 0 & 0 & 0 & 0 & 0 & 0 & 0 & 0 & 0 & 0 & 0 & 0 & 0 & 0 & 0 & 0 & 0 \\ 0 & 0 & 0 & 0 & 0 & 0 & 0 & 0 & 1 & 0 & 0 & 0 & 0 & 0 & 0 & 0 & 0 & 0 \\ 0 & 0 & 0 & 0 & 0 & 0 & 0 & 0 & 0 & 1 & 0 & 0 & 0 & 0 & 0 & 0 & 0 & 0 \\ 0 & 0 & 0 & 0 & 0 & 0 & 0 & 0 & 0 & 0 & 1 & 0 & 0 & 0 & 0 & 0 & 0 & 0 \\ 0 & 0 & 0 & 0 & 0 & 0 & 0 & 0 & 0 & 0 & 0 & 1 & 0 & 0 & 0 & 0 & 0 & 0 \\ 0 & 0 & 0 & 0 & 0 & 0 & 0 & 0 & 0 & 0 & 0 & 0 & 1 & 0 & 0 & 0 & 0 & 0 \\ 0 & 0 & 0 & 0 & 0 & 0 & 0 & 0 & 0 & 0 & 0 & 0 & 0 & 1 & 0 & 0 & 0 & 0 \\ 0 & 0 & 0 & 0 & 0 & 0 & 0 & 0 & 0 & 0 & 0 & 0 & 0 & 0 & 1 & 0 & 0 & 0 \\ 0 & 0 & 0 & 0 & 0 & 0 & 0 & 0 & 0 & 0 & 0 & 0 & 0 & 0 & 0 & 1 & 0 & 0 \\ 0 & 0 & 0 & 0 & 0 & 0 & 0 & 0 & 0 & 0 & 0 & 0 & 0 & 0 & 0 & 0 & 1 & 0 \\ 0 & 0 & 0 & 0 & 0 & 0 & 0 & 0 & 0 & 0 & 0 & 0 & 0 & 0 & 0 & 0 & 0 & 1 \end{bmatrix}$$

The highlighted rows in both matrices indicate the positioning of the respective inflation measures.

- **M3 model**: We consider a standard trend inflation VAR (Ti-VAR) without a common trend inflation factor, inflation expectations and stochastic volatility in the state equation i.e.:

$$\boldsymbol{y}_t = \boldsymbol{\tau}_t + \sum_{l=1}^{p} \mathbf{B}_l \left(\boldsymbol{y}_{t-l} - \boldsymbol{\tau}_{t-l} \right) + \boldsymbol{\varepsilon}_t, \qquad \boldsymbol{\varepsilon}_t \sim \mathcal{N}(\mathbf{0}, \exp(h_t)\boldsymbol{\Sigma}) \tag{D.10}$$

$$\boldsymbol{\tau}_t = \mathbf{S}_{\gamma}\boldsymbol{\gamma} + \mathbf{S}_{\tau\pi}\boldsymbol{\tau}_t^{\pi} \tag{D.11}$$

$$\tau_{jt}^{\pi} = \tau_{jt-1}^{\pi} + \epsilon_{jt}^{\tau\pi}, \quad j = 1, ..., q, \qquad \epsilon_{jt} \sim \mathcal{N}(0, q_{jt}) \tag{D.12}$$

In M3 and all the subsequent (M4 - M7) models the $\mathbf{S}_{\gamma}$ remains unchanged while $\mathbf{S}_{\tau\pi}$ is the following (20×3) matrix:

$$\mathbf{S}_{\gamma} = \begin{bmatrix} 0 & 0 & 0 \\ 0 & 0 & 0 \\ 0 & 0 & 0 \\ 0 & 0 & 0 \\ 0 & 0 & 0 \\ 0 & 0 & 0 \\ 0 & 0 & 0 \\ 0 & 0 & 0 \\ 1 & 0 & 0 \\ 0 & 1 & 0 \\ 0 & 0 & 1 \\ 0 & 0 & 0 \\ 0 & 0 & 0 \\ 0 & 0 & 0 \\ 0 & 0 & 0 \\ 0 & 0 & 0 \\ 0 & 0 & 0 \\ 0 & 0 & 0 \\ 0 & 0 & 0 \\ 0 & 0 & 0 \end{bmatrix}$$

- **M4 model**: This is the proposed Ti-VARe model described in Section 2 but with the following modifications: (i) we use the EWMA filter to proxy inflation expectations, (ii) we set $d_0 = 0$ and $d_1 = 1$ in (4) and (iii) we do not consider stochastic volatility in the error terms of the trend inflation equation (3).

- **M5 model**: This is the same with the M4 model but with the inflation expectation proxies as described in Table 2.
- **M6 model**: This is the M5 model but with stochastic volatility in the error terms of the trend inflation equation (3).
- **M7 model**: This the proposed model as described in Section 2.

Appendix E Additional results

Figure E.7 presents the histogram of the posterior draws of $d_{0,j}$ and $d_{1,j}$ parameters, with $j = PCE, GDPd, CPI$. More specifically, the left column of Figure E.7 shows the posterior distribution of $d_{0,j}$, i.e. the constant term in equation (4) in the main text, which posterior mean is almost equal to zero. On the right hand side of Figure E.7, we show the posterior distribution of the slope coefficient of equation (4), $d_{1,j}$, across inflation metrics. The results suggest that unity is well contained in the 95% confidence interval. Therefore, the hypothesis that the long-run inflation forecasts and the EWMA filter are biased measures of model-based trend inflation, or simply that $d_{0,j} \neq 0$ and $d_{0,j} \neq 1$ does not hold in this study $\forall j$.

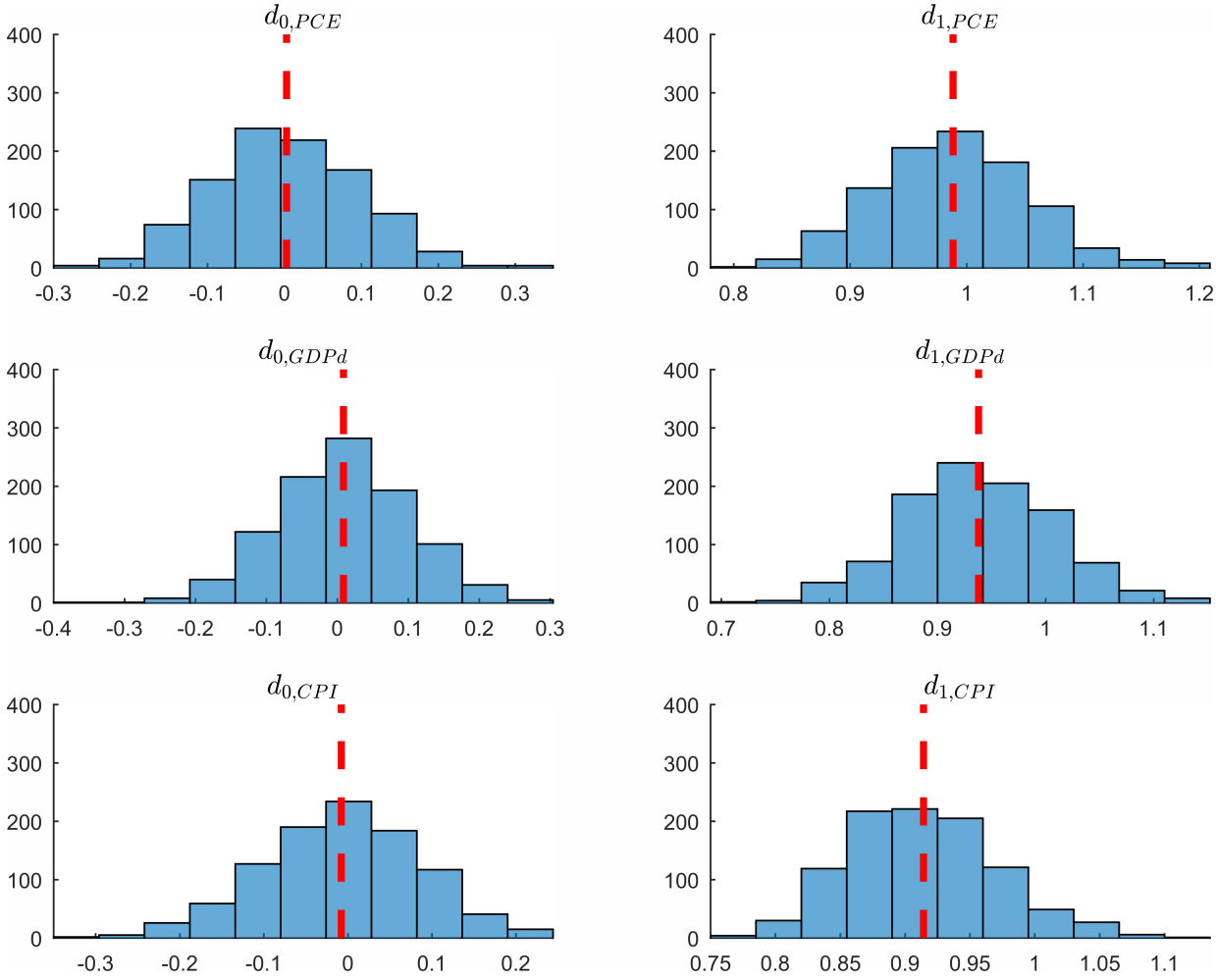

Figure E.7: Histogram of the posterior draws of $d_{0,j}$ and $d_{1,j}$ parameters, with $j = PCE, GDPd, CPI$. The dashed red line denotes the posterior mean.

BANK OF GREECE WORKING PAPERS

343. Angelis, A. and A. Tagkalakis, “Formation, heterogeneity and theory consistency of inflation expectations in the euro area”, June 2025

344. Konstantinou, P., Rizos, A., and A. Stratopoulou, “The effectiveness of macroprudential policies in curbing operational risk exposures”, July 2025

345. Vilerts, K., Anyfantaki, S., Beņkovskis, K., Bredl, S., Giovannini, M., Horky, F. M., Kunzmann, V., Lalinsky, T., Lampousis, A., Lukmanova, E., Petroulakis, F., and K. Zutis, “Details matter: loan pricing and transmission of monetary policy in the euro area”, July 2025

346. Hondroyiannis, G., Papapetrou, E., and P. Tsalaporta, “Exploring the role of technological innovation and fertility on energy intensity: Is a fresh narrative unfolding?”, August 2025

347. Anyfantaki, S., Blix Grimaldi, M., Madeira, C., Malovana, S., and G. Papadopoulos, “Decoding climate-related risks in sovereign bond pricing: a global perspective”, September 2025

348. Brissimis, S. and E. Georgiou, “Assessing the impact of unconventional monetary policy on long-term interest rates in the euro area with the use of a macro-finance model”, September 2025

349. Economides, G., Malley, J., Philippopoulos, A., and A. Rizos, “Policy interventions to mitigate the long run costs of Brexit”, October 2025

350. Angelopoulos, G., Bragoudakis, Z., Dimitriou, D., and A. Tsioutsios, “A new proposal for forecasting inflation in the eurozone. A global model”, October 2025

351. Delikouras, S., Kontinopoulos, A., Malliaropulos, D., and P. Migiakis, “Bond portfolio rebalancing during dash-for-cash events: Evidence from the COVID-19 outbreak”, October 2025.

352. Bragoudakis, Z. and A. Tsioutsios, “Bank concentration and asymmetric interest rate spreads pass through: evidence from selected euro area countries”, November 2025.

353. Andreou, P., Anyfantaki, S., Dellis, K., and C. Makridis, “Doing matters more than knowing: evidence from environmental preferences”, December 2025.

354. Chrysanthakopoulos, C. and A. Tagkalakis, “Natural disasters and the effects of reconstruction expenditure on output”, December 2025.

355. Gazilas, E.T. and Z. Bragoudakis, “Can higher education levels improve tax compliance?”, January 2026.

356. Delis, P. and G. Kontogeorgos, “Outlier-robust evaluation of fixed-event macroeconomic survey expectations”, January 2026

357. Gautier, E, Conflitti, C., Enderle, D., Fadejeva, L., Grimaud, A., Gutiérrez, G., Jouvanceau, V., Menz, J. O., Paulus, A., Petroulas, P., Roldan-Blanco, P., and E. Wieland, “Consumer price stickiness in the euro area during an inflation surge”, February 2026

358. Anyfantaki, S., Giannakidis, H., Malliaropulos, D., Migiakis, P., and F. Petroulakis, “Bond funds' risk taking and monetary policy”, February 2026

359. Karamanis, D., Kotsogiannis, C., and E. Papapetrou, “Threshold-based policies and distortions in housing markets, March 2026